https://doi.org/10.5194/egusphere-2025-4570
Preprint. Discussion started: 5 October 2025

A synthesis of water, energy, and carbon fluxes sensitivity to climate variables in Southeast Asia

Jianning Ren[1], Zhaoyang Luo[1], Xiangzhong Luo[2], Stefano Galelli[3], Athanasios Paschalis[4,5], Valeriy Y. Ivanov[6], Shanti Shwarup Mahto [1,7], Simone Fatichi[1]

[1] Department of Civil and Environmental Engineering, National University of Singapore, Singapore, Singapore

[2]Department of Geography, National University of Singapore, Singapore, Singapore

[3]Department of Civil and Environmental Engineering, Cornell University, Ithaca, USA

[4]Department of Civil and Environmental Engineering, University of Cyprus, Cyprus

[5]Department of Civil & Environmental Engineering, Imperial College London, London, United Kingdom

[6]Department of Civil and Environmental Engineering, University of Michigan, Ann Arbor, USA

[7]Department of Geoinformatics, Central University of Jharkhand, Ranchi, India

Correspondence:

Jianning Ren (jren@nus.edu.sg)

https://doi.org/10.5194/egusphere-2025-4570
Preprint. Discussion started: 5 October 2025

Abstract

Southeast Asia (SEA) plays an important role in the Earth's carbon and water cycle, yet ecohydrology dynamics occurring in this region remain poorly understood due to the paucity of field observations and modelling studies. Here, we investigate water, energy, and carbon fluxes by combining existing flux tower data with mechanistic ecohydrological modelling for 20 sites. A sensitivity analysis to meteorological forcings is used to understand water and energy limitations. Results show large latitudinal differences but overall suggest a strongly energy-limited region, where evapotranspiration (ET) is tightly correlated with net radiation and is highly responsive to relative humidity. Gross primary productivity (GPP) is also correlated to net radiation and is most responsive to shortwave radiation changes. Only a few ecosystems in SEA show signs of water limitations, such as certain grasslands in the Tibetan plateau, savannas, and dry deciduous forests. We further disentangled the relative effect of warming and humidity changes in vapor pressure deficit (VPD). Sensitivity analysis indicates that climate warming-induced VPD changes – rather than pure warming – can have important effects on ET but the opposite is true for GPP with complex GPP responses to temperature based on the thermal photosynthetic optimum and phenological responses. Water use efficiency (WUE) is highly correlated with annual mean precipitation across space, but its responses to precipitation changes are less consistent and WUE changes are most sensitive to relative humidity. Carbon use efficiency (CUE) is more responsive to air temperature than other climate drivers. These insights quantify water, energy, and carbon fluxes in an underrepresented part of the Earth and enhance our understanding of how climate can modify carbon and water cycles in this region.

https://doi.org/10.5194/egusphere-2025-4570
Preprint. Discussion started: 5 October 2025

Key points

- Ecosystems in Southeast Asia are mainly energy-limited, with a few exceptions.
- ET in Southeast Asia is most sensitive to relative humidity changes rather than purely air temperature, while GPP is most responsive to shortwave radiation.
- WUE is most sensitive to relative humidity and CUE is most responsive to air temperature

1 Introduction

Southeast Asia (SEA) is characterized by a very distinct gradient in vegetation cover, going from a dense equatorial forest in Indonesia and Malaysia up to cold-adapted grasslands in the southern Tibetan Plateau (south of 34° N). With its high land-atmosphere CO_2 fluxes, this region plays an important role in Earth's carbon (C) and water cycles (Beer et al., 2010; Sullivan et al., 2020). Yet, the ecohydrology of SEA has historically been understudied due to a combined paucity of field observations and relatively few regional modelling efforts targeted to SEA. Therefore, only few articles exist describing water, energy, and carbon fluxes of ecosystems across SEA (Giambelluca et al., 2016; Huete et al., 2008; Kuricheva et al., 2021; Qian et al., 2019; Song et al., 2017; Tan et al., 2012; Tanaka et al., 2008; Tang et al., 2018; Wang et al., 2022; Zhang et al., 2016), with some broader synthesis for a few sites in Asia (Hirata et al., 2008; Kato & Tang, 2008; Saigusa et al., 2008), but largely missing for the entire SEA region. This hinders the effective evaluation of carbon and water fluxes and prediction of future water availability in SEA (Sirisena et al., 2018; Vu et al., 2023; Yuan Zhang et al., 2016). Furthermore, the expected increase of vapor pressure deficit (Novick et al., 2024), the change in the frequency of extreme weather events,

https://doi.org/10.5194/egusphere-2025-4570
Preprint. Discussion started: 5 October 2025

and the shifts in precipitation patterns under climate change could pose a significant threat to vegetation productivity and its capability to maintain carbon storage (Aadhar & Mishra, 2020; Cervarich et al., 2016; Thirumalai et al., 2017), with SEA being identified as one of the largest sources of uncertainties in the estimation of terrestrial carbon sink (Bastos et al., 2020). It is therefore imperative to understand the sensitivity of these ecosystems to climate variables.

SEA covers an area of approximately 7.5 million km^2 and features a broad climate and vegetation gradient (Estoque et al., 2019; Qian et al., 2019). The majority of this region is affected by a monsoon climate, characterized by two distinct wet and dry seasons (Huete et al., 2008). The wet season of SEA – lasting from June to October for north of the Equator and from November to February for south of the Equator – receives substantial precipitation from the monsoon. On the other hand, the dry season of SEA – extending from December to March for north of the Equator and from June to September for south of the Equator – is marked by prolonged dry spells that typically last more than a week (Wang, 2006). In this study we mostly focused on regions North of the Equator because of data availability and because ~80% of SEA land is located north of the Equator.

The distribution of natural vegetation in SEA is primarily shaped by elevation and latitude (Figure 1). Regions near the Equator are predominantly covered by tropical broadleaf evergreen rainforest, which receive a continuous supply of precipitation with little seasonality (Estoque et al., 2019; Zhang et al., 2016). Large regions of pristine tropical forest have, however, been converted into oil palm and rubber plantations (Vijay et al., 2016; Wang et al., 2023). In contrast, as we move north, the dry season becomes more pronounced, and land cover is characterized by a transition between broadleaf evergreen forests and dry deciduous broadleaf forests in the

https://doi.org/10.5194/egusphere-2025-4570
Preprint. Discussion started: 5 October 2025

lowlands, while evergreen forests persist at higher elevations (Fei et al., 2018). Some large lowland areas have also been converted to agricultural use, with rice and maize being the most commonly cultivated crops (Belton & Fang, 2022; Sun et al., 2023; You et al., 2014). Vast regions are also covered by Southeast Asian savannas, characterized by tropical broadleaf evergreen trees (cover fraction smaller than 45%) and usually C_4 grasses (Pletcher et al., 2022; Ratnam et al., 2016). In these ecosystems, changes in precipitation patterns can largely affect the transpiration rates and vegetation growth (Guan et al., 2015; Stott, 1990). Additionally, the intensity and duration of the summer monsoon vary in response to the Indian and Pacific Ocean dynamics, which can drastically reduce water availability for extended periods (Cook et al., 2010; Nguyen et al., 2020). Therefore, understanding how vegetation responds to climate drivers – such as temperature, relative humidity, precipitation, and solar radiation – is crucial for enhancing our understanding of the ecohydrology of SEA ecosystems and improving predictions of water availability and carbon fluxes in a changing climate.

There are significantly fewer ecohydrology studies in SEA compared to other tropical regions (e.g., Amazon), and little is known about how plants respond to environmental variables and how this response varies across water availability and latitudinal gradients (Huete et al., 2008; Qian et al., 2019; Satriawan et al., 2024; Zhao et al., 2024). Most of the previous studies focused on a specific area or region, making it difficult to generalize the results across larger scales or over the entire SEA (Alberto et al., 2011; Fei et al., 2018; Li et al., 2010; Vu et al., 2023; Yang et al., 2023; Yuan Zhang et al., 2016). For example, using flux tower data, Fei et al. (2018) found that temperature is the main driver of carbon sinks in a tropical forest of SEA, while precipitation is the primary driver in a savanna. Combining different remote sensing

https://doi.org/10.5194/egusphere-2025-4570
Preprint. Discussion started: 5 October 2025

datasets, Zhang et al. (2016) indicated that the GPP of tropical forests is mostly affected by solar radiation during the wet season. Concurrently, Guan et al. (2015) found that GPP of tropical forests decreases with water stress, when the total annual precipitation falls below 2000 mm year^{-1}, suggesting that there are conditions where water availability is still the limiting factor of plant photosynthesis. These findings highlight the need for a deeper understanding and generalization of the mechanisms controlling carbon and water cycle in SEA and the identification of the primary climate drivers (e.g., air temperature, relative humidity, precipitation, solar radiation, and wind speed) across the large latitudinal and vegetation cover gradients of SEA.

Leveraging on a compilation of existing flux tower data, and mostly on the capabilities of a mechanistic ecohydrological model T&C (Fatichi et al., 2012a, 2012b), we conducted a series of numerical experiments (e.g., Fei et al., 2018; Mastrotheodoros et al., 2019) to quantify water, energy, and carbon exchanges in 20 sites across the whole SEA. More specifically, this study addresses the following questions: (i) What are the baseline magnitudes of current ET, GPP, and other ecohydrological variables in terrestrial ecosystems across Southeast Asia? (ii) How do ET, GPP, and other ecohydrological variables respond to perturbations in climate drivers, such as air temperature, relative humidity, precipitation, solar radiation, and wind speed? By addressing these questions, we contribute new knowledge to the ecohydrological functioning of different ecosystems in an understudied region of the Earth.

2 Method

To better understand the landcover types of SEA and to assess whether the available flux tower sites represent the majority of these types, we first reconstructed the

https://doi.org/10.5194/egusphere-2025-4570
Preprint. Discussion started: 5 October 2025

landcover map of SEA based on available remote sensing products. We then set up a mechanistic ecohydrological model for existing flux tower sites and analysed the correlation between ecohydrological variables and climate drivers. Lastly, we conducted virtual experiments in terms of sensitivity analysis to understand the main drivers of ecohydrological variables in SEA.

2.1 Landcover maps of SEA

To better represent the landcover changes of SEA during recent years, we reconstructed a 1 km resolution landcover map for the year of 2022 by elaborating on available land cover maps derived from remote sensing datasets. This includes the databases of: MODIS landcover datasets (MCD12Q1), global forest watch, crop area and types, rubber plantation extent, oil palm plantation extent, and glacier cover area (Table 1). Specifically, we used the MODIS landcover map of year 2022 (Friedl et al., 2002; Friedl et al., 2010) as the base map, then overlaid the forest loss map from global forest watch (Hansen et al., 2013) to extract the cumulative areas that have changed over the last 20 years. Due to the forest watch map having much higher resolution (30m) than MODIS data (500m), we only assume that MODIS landcover pixel is changed when more than 60% of its area has lost forests. For these forest loss areas, we overlapped the crop-related datasets, rubber plantation, and oil palm data to update the MODIS basemap with their corresponding vegetation types.

Table 1. Datasets used for reconstructing a combined landcover map for Southeast Asia

Data	Period	Resolution	Region	References
MODIS landcover (MCD12Q1)	2001-2022	500m	Global	(Friedl et al., 2002; Friedl et al., 2010)
Global forest watch	2000-2022	30m	Global	(Hansen et al., 2013)
Rubber plantation	1993-2016	10m	Southeast Asia	(Wang et al., 2023)
Oil Palm	2019	10m	Global	(Descals et al., 2021)

Oil Palm	2001-2016	100m	Malaysia and Indonesia	(Xu et al., 2020)
Crop area	2003-2019	30m	Global	(Potapov et al., 2022)
Crop types (SPAM 2010)	2010	10km	Global	(You et al., 2014)
Glacier data (GAMDAM)	2018	Polygon	Asia	(Sakai, 2019)

2.2 Flux tower sites

We utilized available data from 20 flux tower sites located across SEA for our analysis and numerical experiments. These flux tower sites span a wide range of latitudes and climate gradients, extending from the Tibetan Plateau to Equatorial regions (Figure 1). The mean annual precipitation across these sites varies from 520 to 4762 mm year^{-1}, whereas the mean annual air temperature ranges from 1.8 ℃ to 28 ℃ (Table 2). The vegetation types include evergreen broadleaf forests (which covers 33.8% of SEA), savannas and woody savannas (15.5%), deciduous broadleaf forest (12.7%), rice field (10.2%), mixed forest (4%), C_3 grasslands (3.6%), mangrove and wetlands (2%), C_4 grasslands (1.4%), evergreen needleleaf forests (1.2%), rubber plantation (0.6%) and montane cloud forests (0.2%). Therefore, the analysed sites cover all of the main vegetation types of SEA, except for oil palm and maize, which account for 3% and 3.5% of land cover in SEA, respectively. Detailed information on the 20 flux tower sites and associated references is provided in Table 2.

Due to the large uncertainties in energy flux measurements (e.g., leading to energy closure problems, as in Table 2) with most observations collected in complex environmental conditions, the lower quality standardization protocols for raw data processing for some of the sites, as compared to standards assumed in Fluxnet-2015 (Pastorello et al., 2020), and the numerous data gaps, we treat the observed fluxes

https://doi.org/10.5194/egusphere-2025-4570
Preprint. Discussion started: 5 October 2025

only as an indication of model performance. Instead, we rely on simulations of a well-tested ecohydrological model to compute all the long-term means and statistics.

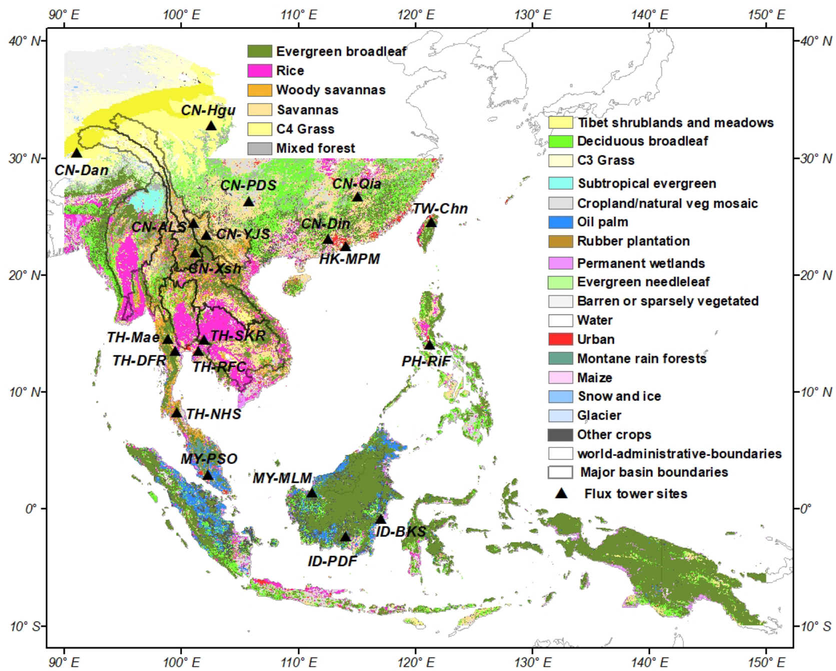

Figure 1. The reconstructed landcover map of Southeast Asia for year 2022 and locations of flux tower sites used for studying the carbon and water cycles in this region. We include the southern part of the Tibetan region because it is the source area of the Mekong and Salween rivers.

Table 2. Characteristics of flux tower sites. These characteristics include the main biome, latitude, longitude, elevation, measurement available period, mean annual precipitation (P_r), mean air temperature (T_a), mean short wave radiation (R_{sw}), mean vapor pressure deficit (VPD), mean relative humidity (R_h), and energy balance closure (EC) calculated as the average of the sum of latent heat and sensible heat fluxes normalized by net radiation at daily scale, and references of original studies for these flux tower sites.

https://doi.org/10.5194/egusphere-2025-4570
Preprint. Discussion started: 5 October 2025

Site	Name	Biome	Lat	Long	Ele (m a.s.l.)	Period	Mean P_r (mm year^{-1})	T_a (°C)	R_{sw} (W m^{-2})	VPD (Pa)	R_h (%)	EC (%)	References
ID-PDF	Palangkaraya drained forest	Tropical forest	-2.345	114.04	30	2002-2005	2331	26.3	198	791	78	85	(Hirano et al., 2007)
ID-BKS	Bukit Soeharto	Tropical forest	-0.83	117.05	20	2001-2002	2276	26.5	169	567	84	40	(GAMO, 2005)
MY-MLM	Maludam	Tropical peat swamp forest	1.45	111.15	3	2014-2015	2902	27.1	202	351	90	NA	(Busman et al., 2023)
MY-PSO	Pasoh Forest Reserve	Tropical forest	2.966	102.3	100	2003-2009	1865	25.3	198	629	81	99	(Takanashi et al., 2010)
TH-NHS	Nakhon_Si	Rubber plantation	8.32	99.58	200	2017-2018	2827	26.4	186	565	84	103	(Unjan et al., 2017)
TH-RFC	Rubber Flux Chachoengsao	Rubber plantation	13.57	101.46	69	2015-2018	1467	27.6	205	785	79	97	(Kanpanon et al., 2015)
TH-DFR	Dry Dipterocarp Forest Ratchaburi	Tropical dry deciduous	13.58	99.50	118	2015-2017	1405	27.2	212	1005	72	100	(Sanwangsri et al., 2017)
PH-RiF	Philippine_Rice Institute flooded	Crop rice	14.14	121.26	27	2012-2014	2729	26.5	180	880	75	81	(Alberto et al., 2014)
TH-SKR	Sakaerat	Tropical dry deciduous	14.49	101.91	543	2001-2003	1483	24.2	198	943	69	87	(Ichii et al., 2017)
TH-Mae	Mae Klong	Tropical dry deciduous	14.57	98.84	231	2003-2004	1361	24.8	202	1004	69	NA	(Ichii et al., 2017)
CN-Xsh	Xishuangbanna	Subtropical evergreen broadleaf	21.95	101.20	756	2003-2005	1312	21.2	149	614	76	52	(Zhang et al., 2006)
HK-MPM	Mai Po Mangrove	Mangrove	22.49	114.03	0	2016-2018	1843	23.7	164	645	77	97	(Liu & Lai, 2019)
CN-Din	Dinghushan	Subtropical evergreen broadleaf	23.17	112.53	300	2003-2005	1374	20.4	139	669	71	47	(Wang et al., 2006)
CN-YJS	YuanJiang	Savanna with C_4 grass	23.47	102.17	553	2013-2015	630	24.2	195	1370	57	52	(Fei et al., 2017)
CN-ALS	AiLaoShan	Mixed forest	24.54	101.03	2500	2009-2013	1890	11.6	158	326	74	100	(Song et al., 2017)
TW-Chn	ChiLan mountain	Montane cloud forest	24.58	121.4	1650	2007-2009	4763	14.5	116	138	91	120	(Hsieh et al., 2008)
CN-PDS	Puding	Savanna with C_4 grass	26.35	105.75	1170	2015-2019	1327	16.3	133	429	79	47	(Wang et al., 2020)
CN-Qia	Qianyanzhou	Evergreen needleleaf	26.74	115.06	109	2003-2005	1170	18.2	141	702	72	78	(Yu et al., 2008)
CN-Dan	Dangxiong	Grassland C_3	30.49	91.06	4330	2004-2005	520	2.2	221	404	42	126	(Shi et al., 2006)
CN-Hgu	Hongyuan	Grassland C_3	32.84	102.59	3500	2015-2017	778	3.0	206	325	62	110	(Peng et al., 2021)

https://doi.org/10.5194/egusphere-2025-4570
Preprint. Discussion started: 5 October 2025

2.2 Mechanistic ecohydrological model

We utilized the mechanistic ecohydrological (terrestrial biosphere) model T&C, which resolves the coupled dynamics of water, energy, and carbon fluxes at the land surface at the hourly scale (e.g., Fatichi et al., 2012a, 2012b; Mastrotheodoros et al., 2019; Meili et al., 2024; Paschalis et al., 2024). Specifically, T&C simulates the hydrological processes including canopy interception and evaporation, transpiration, ground evaporation, infiltration, surface runoff and subsurface lateral and vertical flow (Mastrotheodoros et al., 2020). In addition, it simulates dynamic vegetation processes, including photosynthesis, carbon allocation to different plant compartments (e.g., leaves, sapwood, hardwood, fine roots), respiration, and tissue turnover, at daily scales. T&C also simulates phenology based on a multi-criteria scheme which considers the effect of temperature, soil moisture, incoming radiation, and length of the photoperiod (Fatichi et al., 2012a).

We used the observational data from 20 flux towers to compare with T&C simulations across these sites and identify suitable parameters. We then used hourly meteorological forcing observed at the flux towers (ranging from 1 to 7 years) as a baseline climate inputs for the numerical experiments. The T&C model has been widely applied and tested across various climate and ecosystems (Fatichi et al., 2014; Z. Luo et al., 2024; Manoli et al., 2018; Meili et al., 2024; Moustakis et al., 2022; Pappas et al., 2016) and it is further tested here. A detailed description of T&C model can be found in the aforementioned publications.

2.3 Numerical simulations and perturbation experiments

We began by performing a correlation analysis to examine the relationship between ecohydrological variables (at annual scales) including ET, GPP, water use efficiency

https://doi.org/10.5194/egusphere-2025-4570
Preprint. Discussion started: 5 October 2025

(WUE, calculated as GPP/Transpiration), carbon use efficiency (CUE, calculated as GPP/NPP with NPP being the net primary productivity) and key climate drivers (i.e., annual mean air temperature T_a, relative humidity R_h, short wave radiation R_{sw}, net radiation R_n, precipitation P_r, and wind speed W_s). Following this analysis of the simulations for the current climate, we conducted numerical experiments to investigate how ecohydrological variables respond to the changes in climate drivers such as air temperature, relative humidity, precipitation, solar radiation, and wind speed. As all these variables have different temporal variability and units – in order to make the responses of ecohydrological fluxes comparable across different climate drivers perturbations for a given location and across locations – we adjusted the climate inputs by increasing or decreasing them by one and two standard deviations (SD) of the magnitude of interannual variability (Mastrotheodoros et al., 2019). Given that most flux towers have data of less than five years (Table 2), we used ERA5 hourly data over 1981-2022 (Hersbach et al., 2020) to obtain the annual means of meteorological variables to calculate the annual SD over the 41 years of ERA5 product for each variable. The SD of each climate variable is a single value for the entire record. From the ERA5 dataset, we extracted air temperature at 2-meter height, wind speed components at 10 meters, dew point temperature at 2 meters, and mean surface downward shortwave radiation. ERA5 precipitation has limitations and is deemed less reliable in tropical regions (Lavers et al., 2022). Therefore, we used precipitation data obtained from the Climate Hazards Group Infrared Precipitation with Stations (CHIRPS, Funk et al., 2015).

In the perturbation experiment, we modified the time series of each climate variables by applying four scenarios that shifted the mean of the resulting time series by one or two SDs relative to the original. Specifically, we perturbed each climate variable by

https://doi.org/10.5194/egusphere-2025-4570
Preprint. Discussion started: 5 October 2025

adding/subtracting or multiplying by a scaling factor using: (i) plus one and (ii) two SDs and (iii) minus one and (iv) two SDs of the original climate variables. Daily cycles and seasonal variability are thus just shifted by these perturbation values. For perturbation of solar radiation, we adjust the direct and diffuse radiation proportionally, applying the same SDs change to both. As most of the flux tower sites have observations for only two or three years (Table 2), which may cause the results to be strongly influenced by the initialization of vegetation carbon pools, we ran the perturbation and the baseline experiments for all 20 sites for the same length of six years, which is twice of the average length of all flux tower sites, by repeating the available meteorological inputs in a concatenated sequence. Then we calculate the difference between the perturbed scenarios and the baseline to analyse the sensitivity of ecohydrological variables to climate drivers.

Air temperature changes affect relative humidity and vapor pressure deficit (VPD). To disentangle their individual effects, we tested three different methods of perturbing air temperature: (i) we change the air temperature, but do not change the relative humidity; (ii) we change the air temperature, but we do not change the vapor pressure, so the relative humidity is modified; (iii) we change the air temperature, but we do not change the VPD, so both relative humidity and vapor pressure are different. Out of the three different methods, method (iii) can represent the most direct air temperature effect because it keeps VPD the same. The other two methods represent a combined effect of perturbed air temperature and VPD, because VPD changes with air temperature. It changes more in the method (ii) as vapor pressure is not allowed to increase. More detailed equations for the three perturbation methods can be found in supplementary material section S1.

https://doi.org/10.5194/egusphere-2025-4570
Preprint. Discussion started: 5 October 2025

3 Results

3.1 Model validation

The energy and carbon fluxes, including net radiation (R_n), sensible heat (H), latent heat (LE), and GPP, are used to validate the T&C model. Considering the very large uncertainty in the data, the model performance is generally good in capturing these fluxes across 20 sites (Table 3, Figure 2, Figure S1, S2 and S3) with few exceptions. The seasonality of simulated energy fluxes is generally well matched with observations except for certain nonseasonal sites such as ID-BKS and MY-MLM (Figure 2). There are also many stations that do not report GPP as the Net Ecosystem Exchange observations were not processed; however, for sites where data are available, the model can capture the seasonality and magnitude of GPP generally well, except for MY-MLM and CH-YJS (Figure S3, Table 3). Given the short duration and the limited quality of flux-tower observations in certain challenging ecosystems, see for instance the large lack of energy balance closure (Table 2), we consider the overall model skill satisfactory for the objective of the study.

https://doi.org/10.5194/egusphere-2025-4570
Preprint. Discussion started: 5 October 2025

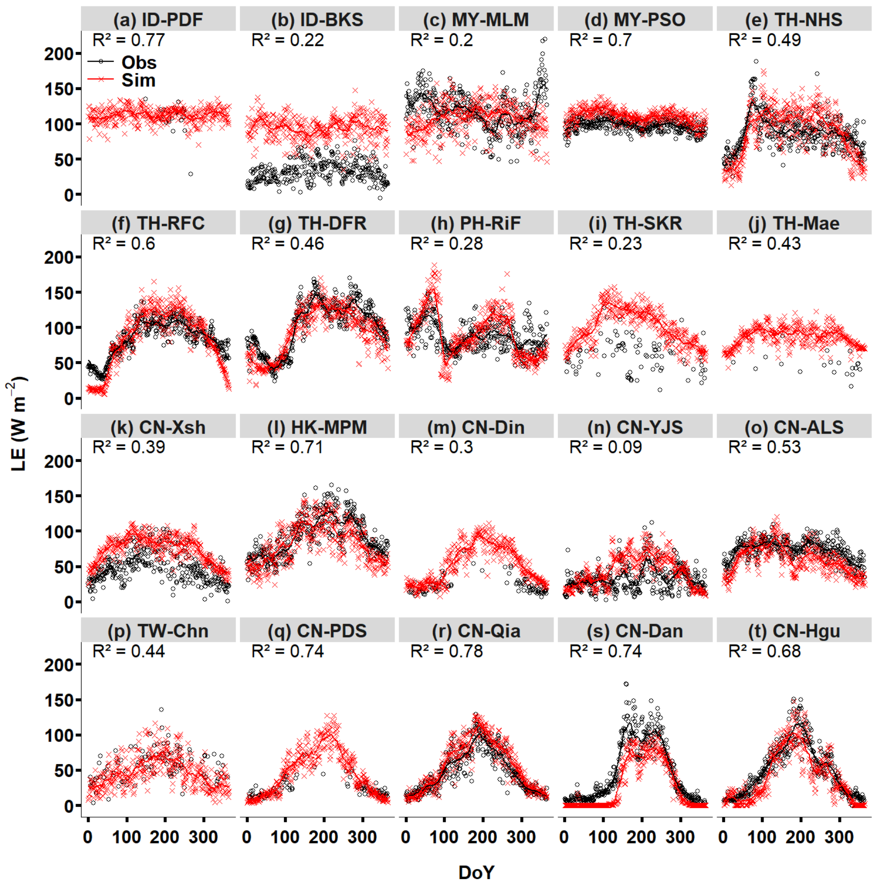

Figure 2. Comparison of T&C model simulation with latent heat (LE) data from flux towers. The mean daily latent heat is calculated for every day of year (DoY) considering all of the years with observations. We also applied a moving average method with a window of 30 days to calculate the smoothed seasonality (the continuous line) of observed and simulated LE. Coefficient of determination (R^2) of simulated vs. observed LE at the daily scale are shown at the top left for each site.

Table 3. Coefficient of determination (R^2) between the simulated and observed daily energy and carbon fluxes for 20 flux sites. NA indicates no data available from flux tower sites.

Flux sites	Net radiation	Latent heat	Sensible heat	GPP
ID-PDF	0.9	0.77	0.18	NA
ID-BKS	0.42	0.22	0.21	NA
MY-MLM	NA	0.2	0.17	0.22
MY-PSO	0.94	0.7	0.56	NA
TH-NHS	0.61	0.49	0.005	0.54

https://doi.org/10.5194/egusphere-2025-4570
Preprint. Discussion started: 5 October 2025

TH-RFC	0.55	0.6	0.46	0.59
TH-DFR	0.54	0.46	0.47	0.48
PH-RiF	0.52	0.28	0.53	0.67
TH-SKR	0.88	0.23	0.34	NA
TH-Mae	0.91	0.43	NA	NA
CN-Xsh	0.87	0.39	0.1	NA
HK-MPM	0.95	0.71	0.58	0.54
CN-Din	0.08	0.3	0.01	0.35
CN-YJS	0.83	0.09	0.19	0.14
CN-ALS	0.88	0.53	0.25	0.51
TW-Chn	0.92	0.44	0.69	NA
CN-PDS	0.97	0.74	0.46	0.78
CN-Qia	0.98	0.78	0.61	0.82
CN-Dan	0.91	0.74	0.49	0.66
CN-Hgu	0.65	0.68	0.1	NA

3.2 Correlation analysis

We analyse the correlation between simulated ET and GPP (Table 4, Figure 3) and various climate drivers across the 20 sites. At annual scale and across sites, ET exhibits the strongest correlation with net radiation (Figure 3d, $R^2 = 0.73$), while it shows relatively weaker correlations with precipitation ($R^2 = 0.2$) and wind speed ($R^2 = 0.16$). ET increases with air temperature ($R^2 = 0.55$) in general, though the correlation is weaker as compared with simulated net radiation (Figure 3a). As net radiation is a model output, ET is directly conditioned upon it and there is circularity in its effects on ET. As a result, the air temperature has the strongest correlation with ET among the independent input variables. This remarks how SEA is primarily an energy-limited region and precipitation has only an influence on high latitudes sites in the Tibetan plateau, which tend to be both temperature and water-limited, contrary to most of the other sites below 20º latitude (Figure 3e), which do not show evidence of water limitations at the annual scale.

Unlike other climate drivers, across sites wind speed has a negative correlation with ET because these high wind speed sites are predominantly located in high latitudes

https://doi.org/10.5194/egusphere-2025-4570
Preprint. Discussion started: 5 October 2025

and especially the Tibetan plateau, where ET is much lower (Figure 3f). The low ET values are not caused by high winds, but the covariation of wind with other climate variables leads to this negative correlation pattern. In summary, at the annual scale sites across SEA are largely energy-limited, with a few exceptions usually located at higher latitude.

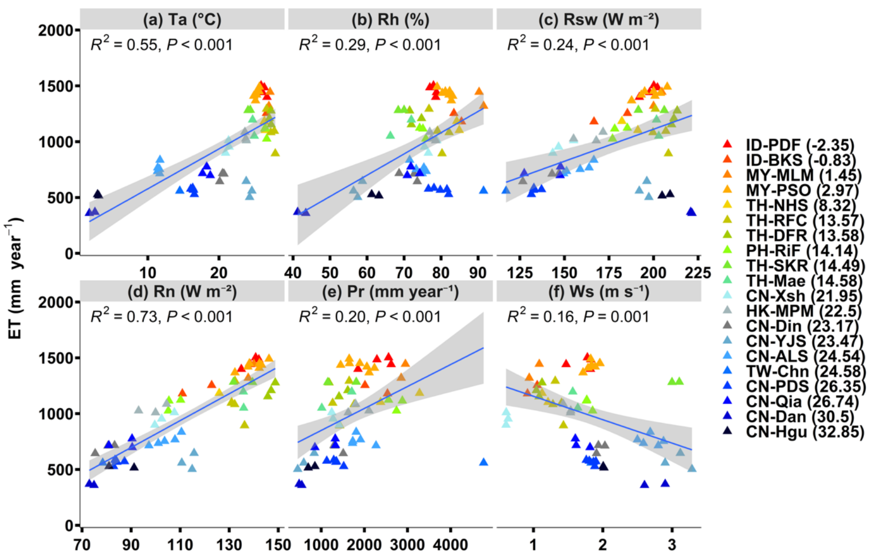

Figure 3. Correlation between annual climate drivers and simulated annual ET across sites. Data points are color-coded to represent flux tower sites at different latitudes. The grey band indicates the 95% confidence intervals of the linear regression line.

Table 4. Flux sites characteristics from T&C model simulations at mean annual scale include evapotranspiration (ET), net radiation (R_n), sensible heat (H), latent heat (LE), gross primary productivity (GPP), and Evaporative ratio (ET/P_r).

Flux Sites	ET (mm year^{-1})	Rn (W m^{-2})	H (W m^{-2})	LE (W m^{-2})	GPP (gC m^{-2} year^{-1})	Evaporative ratio
ID-PDF	1457	139	23	112	3190	0.63
ID-BKS	1217	117	20	94	2861	0.53
MY-MLM	1382	139	28	107	3475	0.48
MY-PSO	1432	140	26	110	3247	0.77

https://doi.org/10.5194/egusphere-2025-4570
Preprint. Discussion started: 5 October 2025

TH-NHS	1143	128	38	88	2852	0.40
TH-RFC	1059	133	50	81	2284	0.72
TH-DFR	1213	147	51	93	2840	0.86
PH-RiF	1088	107	14	91	1655	0.40
TH-SKR	1282	136	34	99	2859	0.86
TH-Mae	1124	136	47	87	2315	0.83
CN-Xsh	954	103	26	74	2527	0.73
HK-MPM	1041	99	14	82	2801	0.56
CN-Din	691	80	24	53	1596	0.50
CN-YJS	569	114	69	44	908	0.90
CN-ALS	761	104	42	60	2359	0.40
TW-Chn	559	78	33	43	1867	0.12
CN-PDS	566	84	40	44	1205	0.43
CN-Qia	730	87	29	56	1876	0.62
CN-Dan	364	74	49	29	341	0.70
CN-Hgu	522	86	44	41	795	0.67

GPP across sites remains strongly correlated with net radiation ($R^2 = 0.55$), but the correlation coefficients are smaller as compared to ET (Figure 4d). In contrast to ET, GPP is not strongly related to shortwave radiation; this is mostly due to a few sites in the Tibetan plateau that have very low GPP (temperature and water-limited), despite receiving high loads of shortwave radiation (Figure 4c). These sites are, however, characterized by proportionally higher sensible heat and lower net radiation (Table 4). At latitudes lower than 24º the correlation between GPP and shortwave radiation is stronger ($R^2 = 0.13$). Moreover, GPP has a stronger correlation ($R^2 = 0.44$) with

https://doi.org/10.5194/egusphere-2025-4570
Preprint. Discussion started: 5 October 2025

relative humidity than ET (Figure 4b). Lower relative humidity leads to higher VPD which induces stomatal closure (Sabot et al., 2022) and thus less photosynthesis given other conditions are the same; this affects GPP more than ET as the latter is still mainly driven by the higher VPD compensating for the stomatal closure. Higher relative humidity sites have also more cloud cover and diffuse light to plants which enhances light use efficiency (Figure S4, Xu et al., 2023). GPP also showed a relatively weak correlation with air temperature, especially for tropical and subtropical sites where higher temperatures do not lead to more GPP (Figure 4a). This suggests that for these tropical and subtropical sites, the temperature for growth has reached its optimum in the model simulations and GPP is limited by other factors, such as radiation and humidity. In summary, GPP in SEA exhibits less climate driven relationships compared to ET, which are largely mediated by humidity and radiation at lower latitudes with temperature and precipitation playing a more pronounced role for a few sites as CN-YJS, CN-Dan, and CN-Hgu.

https://doi.org/10.5194/egusphere-2025-4570
Preprint. Discussion started: 5 October 2025

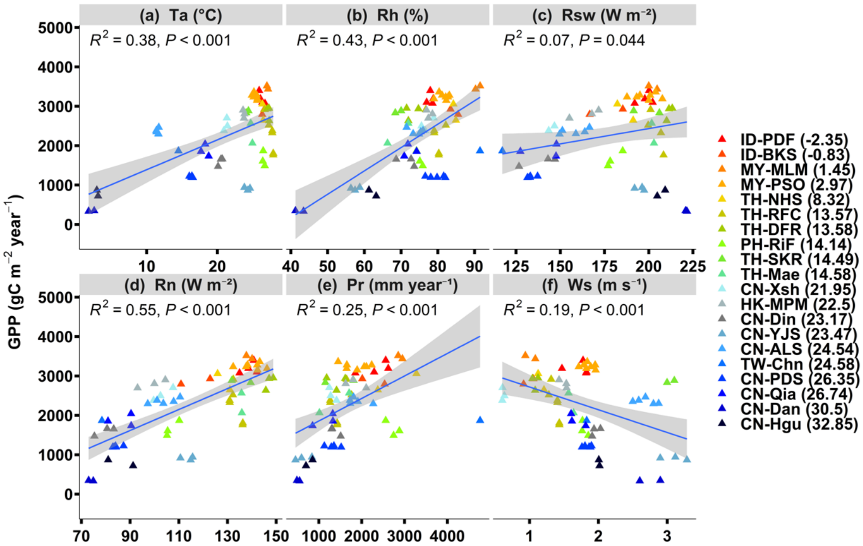

Figure 4. Correlation between annual climate drivers and simulated annual GPP across sites. Data points are color-coded to represent flux tower sites at different latitudes. The grey band indicates the 95% confidence intervals of the linear regression line.

WUE is strongly correlated with precipitation, with higher precipitation leading to larger WUE (Figure 5e). Moreover, it does not exhibit correlation with net radiation, which is very different from the behaviours of ET and GPP (Figure 5d). WUE also shows a very weak and not statistically significant correlation with air temperature and shortwave radiation. The correlation analysis suggests that plants in wetter regions have a higher WUE (at annual scales) than those in drier regions, following global patterns (Fatichi et al., 2023). Additionally, the rice field (PH-RiF) and swamp forest (MY-MLM) exhibit a much higher WUE (Figure 5e), which is due to the very high relative humidity suppressing the transpiration during the growing season (Table 2).

https://doi.org/10.5194/egusphere-2025-4570
Preprint. Discussion started: 5 October 2025

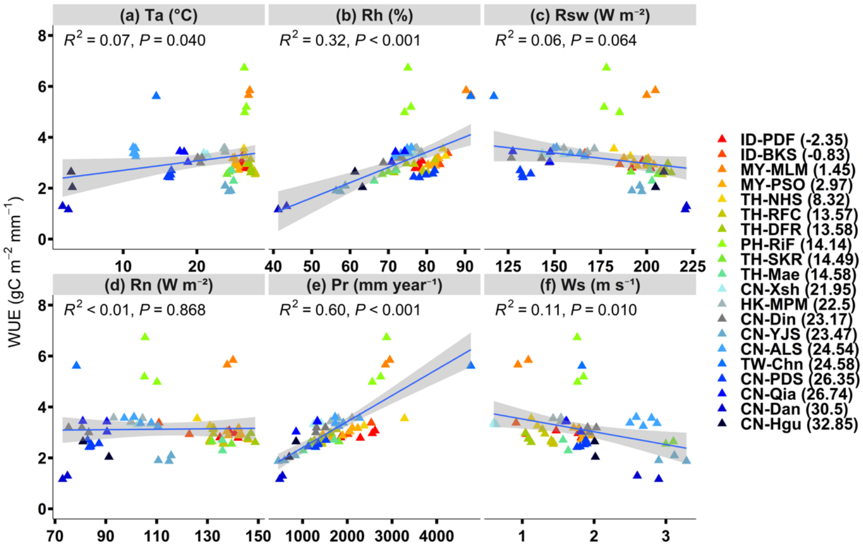

Figure 5. Correlation between annual climate drivers and simulated annual WUE across sites. WUE is calculated as the ratio between annual GPP and transpiration. Data points are color-coded to represent flux tower sites at different latitudes. The grey band indicates the 95% confidence intervals of the linear regression line.

CUE shows a relatively weak correlation with all climate variables with air temperature having the highest correlation (R^2 = 0.24) and no correlation with precipitation and relative humidity (p-value>0.05, Figure 6). CUE generally decreases with higher temperatures, as higher temperature exerts a higher toll on plant maintenance respiration leaving less carbon for growth. Moreover, CUE also decreases with increasing shortwave radiation, although the correlation is relatively weak. These findings are consistent with recent global studies that CUE generally decreases with higher light availability and temperature (Luo et al., 2025). However, the weak correlations between CUE and climate drivers indicates that carbon use efficiency tends to be quite stable across climates and ecosystems (De Lucia et al., 2007).

https://doi.org/10.5194/egusphere-2025-4570
Preprint. Discussion started: 5 October 2025

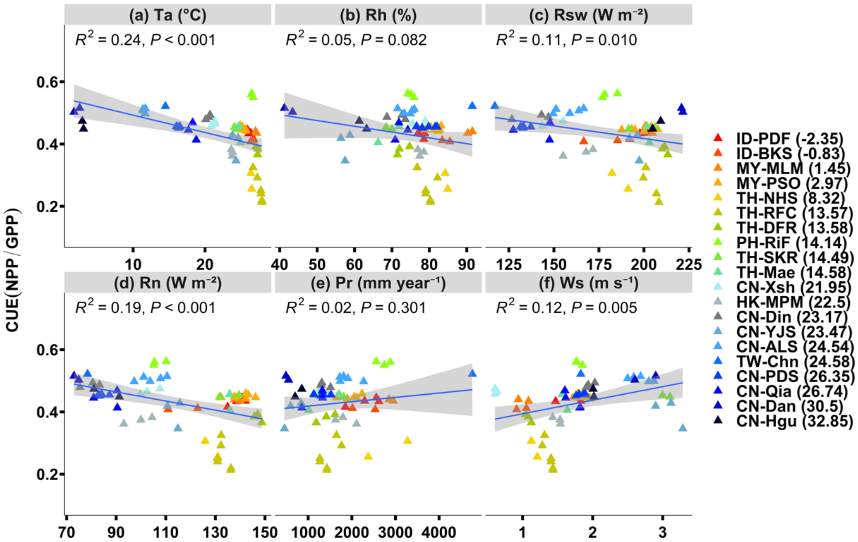

Figure 6. Correlation between annual climate drivers and simulated annual CUE across sites. Data points are color-coded to represent flux tower sites at different latitudes. The grey band indicates the 95% confidence intervals of the linear regression line.

3.3 Sensitivity of ET to climatic variables in the perturbation experiments

The pure effect of modifying air temperature (from method iii) has a small influence in changes in ET, with most of the responses being within ±50 mm year^{-1}, (± 5%), while modifying relative humidity has the strongest effects, with most of the responses spanning within a range of ±125 mm year^{-1} (± 12%) with a largely linear response (Figure 7). Regarding relative humidity changes, the most responsive sites are the CN-ALS mixed forest (2.1% decrease of ET for 1% increase in R_h) and TW-Chn montane cloud forest (2.7% decrease of ET for 1% increase in R_h, Table S1), both located in high-elevation mountain regions with very low VPD baseline and sufficient precipitation (Figure 7I, Table 2). In contrast, the least sensitive site is CN-YJS, with almost no responses (~0.2% decrease of ET for increase 1% in R_h) to relative humidity changes, which is characterized by dry and water-limited conditions

https://doi.org/10.5194/egusphere-2025-4570
Preprint. Discussion started: 5 October 2025

(Figure 7G, Table S1). Although CN-YJS (valley) and CN-ALS (mountain) are located at similar latitudes and relatively close to each other, elevation and associated differences in water availability play a fundamental role in shaping their different responses to climate.

The different ways of perturbing specific humidity associated with a change in air temperature have distinct effects on the ET responses (Figure S5), with method (ii) having the strongest effect (with a range around ±150 mm year^{-1}) as it generates the largest VPD change, which reflects on ET. However, as highlighted by the different perturbation methods, this is mostly a VPD effect rather than a pure air temperature change. Modifying purely air temperature causes many tropical and subtropical sites to even have a decrease of ET with higher air temperatures (Figure S5). This decreasing trend is because plants operate beyond the optimal temperature for photosynthesis and with higher temperatures there is a decrease of GPP and consequently LAI, which leads to smaller ET (Huang et al., 2019).

Shortwave radiation also has a relatively significant effect because most of the responses span a range of ±100 mm year^{-1} (± 10%), and almost all sites show increased ET with a higher shortwave radiation (Figure 7D). The TW-Chn cloud montane forest, which is very limited by light availability, shows the largest responsiveness to changes in solar radiation (~0.8% for 1 W m^{-2}), while the Savanna with C_4 grasses (CN-YJS) is the least affected (0.09% for 1 W m^{-2}, Figure 7I and Table S1), as it is largely water-limited. This confirms that the TW-Chn has the strongest energy limitations because of its persistent cloud cover and extremely high relative humidity with an annual average R_h= 91%, larger than tropical forests. Regarding wind speed, most sites exhibit minimal responses (with a range of smaller than 3% and 50 mm year^{-1} Figure 7E, J), except for the PH-RiF and HK-MPM sites

https://doi.org/10.5194/egusphere-2025-4570
Preprint. Discussion started: 5 October 2025

(larger than 7% for 1 m s^{-1} changes in W_s). Both sites, a flooded rice field and a mangrove, have ponding water at the surface for large period of times, a higher wind speed reduces aerodynamic resistance below the canopy, which can enhance ET especially from the ponding water surface.

ET sensitivity to precipitation varies significantly across different sites (Figure 7H). Most sites located south of 14° N latitude show minimal response (smaller than 1% for 100 mm $year^{-1}$ change in P_r) to changes in precipitation (Figure 7H, Table S1). In contrast, sites on the Tibetan Plateau such as the C_3 grasslands (CN-Dan and CN-Hgu) and the Savanna (CN-YJS) are very sensitive to precipitation changes (larger than 3% for 100 mm $year^{-1}$ changes in P_r), showing that water limitations are shaping the functioning of the ecosystem. Overall, the sensitivity analysis supports the finding that SEA at large is much more energy-limited than water-limited with changes in shortwave radiation and mostly relative humidity affecting ET at almost all of the sites, with precipitation being important only at specific sites.

https://doi.org/10.5194/egusphere-2025-4570
Preprint. Discussion started: 5 October 2025

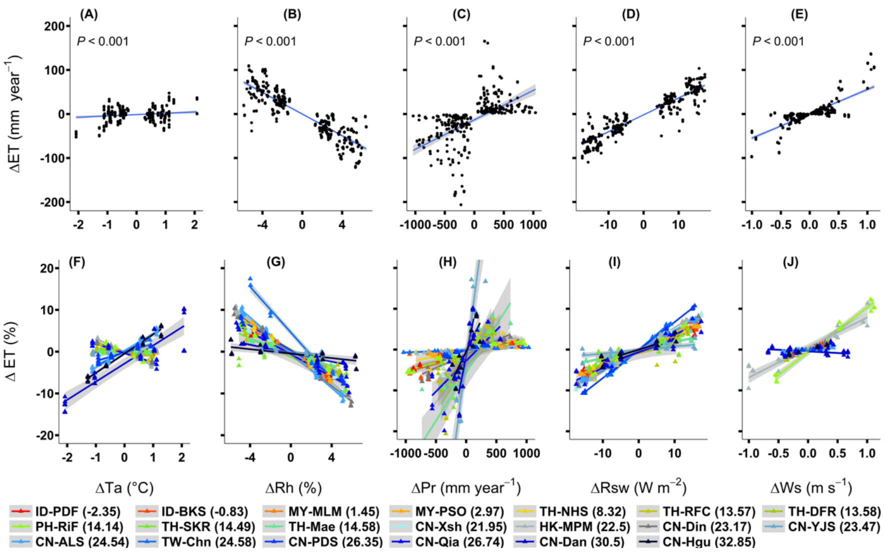

Figure 7. ET responses to perturbation of various climate drivers, including air temperature, relative humidity, precipitation, shortwave radiation, and wind speed. The top panels show the absolute changes of ET, and the bottom panels show the relative changes of ET in percentage. The air temperature perturbation with method (iii) is reported to isolate the pure air temperature effect. Note that some of the extreme points beyond the plotting range are not shown for visual clarity; however, all data points were included in the regression fit.

3.4 Sensitivity of GPP to climatic variables in the perturbation experiments

The responses of GPP to perturbations of climate drivers are more complex and less consistent across different sites compared to ET (Figure 8). For the air temperature effect, almost all the tropical and subtropical sites (south of 22.5° N) show a decrease in GPP with warmer air temperatures (Figure 8F, Table S2). In the simulations, additional warming at these high temperatures is moving vegetation away from thermal optimum which is generally close to 28-29 °C for tropical regions (Huang et al., 2019; Tan et al., 2017). Even though this effect is still debated in the literature (Carter et al., 2024; Doughty et al., 2023; Smith et al., 2020), it seems plausible that GPP decreases at temperatures higher than 28ºC, even though thermal acclimation – not accounted for in the T&C model – might mitigate this effect (Liu et al., 2024;

https://doi.org/10.5194/egusphere-2025-4570
Preprint. Discussion started: 5 October 2025

Oliver et al., 2025; Zarakas et al., 2024). For regions north of 22.5° N, GPP generally increases with warmer temperature, which is due to the simulated extended growing season of about 9 to 18 days, promoting GPP despite water limitations, as also supported by empirical evidence (Grossiord et al., 2022). There is only one exception, the CN-YJS savanna, where GPP declines with warmer temperature. This is due to an enhancement of water stress, which is the dominant factor, since this site is warm and dry (Table 2).

The pattern of GPP responses to air temperature changes is also consistent across different methods of perturbing the air humidity associated with a temperature change (Figure S6, Table S2). However, with method (ii), which produces the largest VPD change, the magnitude of the GPP change is larger. In this case, the cooler temperatures, which are tending toward the optimal range can lead to enhanced photosynthesis and lower VPDs which further promote stomatal opening and photosynthesis and lead to higher GPP (Figure S6 B and E, Doughty et al., 2023; Igarashi et al., 2015; Zarakas et al., 2024). For example, the GPP of sites TH-DFR decreases 123 gC m^{-2} (4.3%) for every 1° increase in air temperature with method (iii), but decreases 206 gC m^{-2} (7%) in the method (ii) (Table S2). The differences of GPP between method (ii) and method (iii) show that the temperature can have a strong effect on photosynthesis regardless of VPD for tropical and subtropical regions. On the other hand, GPP of a strongly thermally limited site as CN-Hgu increases 135 gC m^{-2} (13%) for every 1° increase in air temperature in the method (iii), but only increases 79 gC m^{-2} (7%) in the method (ii) as again higher VPD, which causes stomatal closure and higher water stress counteracts the positive warming effect on growing season length and photosynthesis rates.

https://doi.org/10.5194/egusphere-2025-4570
Preprint. Discussion started: 5 October 2025

GPP is most responsive to radiation changes with a range of ± 170 gC m^{-2} $year^{-1}$ for absolute changes and ±7.5% for relative changes (Figure 8 D and I). GPP generally increases with higher solar radiation except for certain dry or cold regions such as CN-YJS, CN-Dan, and CN-Hug (Figure 8I). More radiation enhances light availability for photosynthesis and increase GPP. For instance, in tropical and sub-tropical regions (south of 22.5°N) reducing shortwave radiation leads to lower GPP, as less light is available for photosynthesis in these dense canopies. Colder regions in the Tibetan plateau have sparse canopies and are already receiving quite a high solar radiation load and the declines trend suggests that these sites do not benefit from higher light availability (Figure 8I). The reduction in GPP at colder sites is an indirect effect due to increased ET driven by higher energy available, which further decreases soil moisture and lengthen the period when plants experience water stress. This occurs also in the CN-YJS savanna, where GPP decreased in response to both higher air temperature and solar radiation. This is the most water-limited ecosystem among those analysed, with only 630 mm $year^{-1}$ of precipitation and potential ET of 2587 mm $year^{-1}$ and thus very vulnerable to drought conditions (Table 2).

The pattern of GPP responses to precipitation is similar to those of ET, with only the drier sites (CN-Dan, CN-Hgu, CN-YJS) being sensitive with a 38 - 107 gC m^{-2} $year^{-1}$ (4.4 -11.9%) increase in GPP for every 100 mm $year^{-1}$ changes in precipitation (Table S2), while most other sites have a change smaller than 2%, mostly controlled by leaf wetness impacting photosynthesis (Figure 8H). The wind speed has a relatively small effect; most of the sites have GPP changes smaller than 2 % for every 1 m s^{-1} increase in wind speed (Figure 8J, Table S2). Higher wind speed generally causes more GPP, which is due to a lower aerodynamic resistance and leaf-boundary layer resistance leading to higher CO_2 diffusion rate and enhanced photosynthesis rate (Damour et al.,

https://doi.org/10.5194/egusphere-2025-4570
Preprint. Discussion started: 5 October 2025

2010; Fatichi et al., 2023). Relative humidity also has a relatively small effect on GPP (with a range of ±40 gC m^{-2} and ±5%) but higher than wind speed (a range of ±25 gC m^{-2} and ±2.5%), with most sites increasing GPP with higher relative humidity, particularly for the dry sites we mentioned earlier. This is due to higher relative humidity (lower VPD) which leads to stomata opening and allows for higher CO_2 uptake and thus enhances GPP.

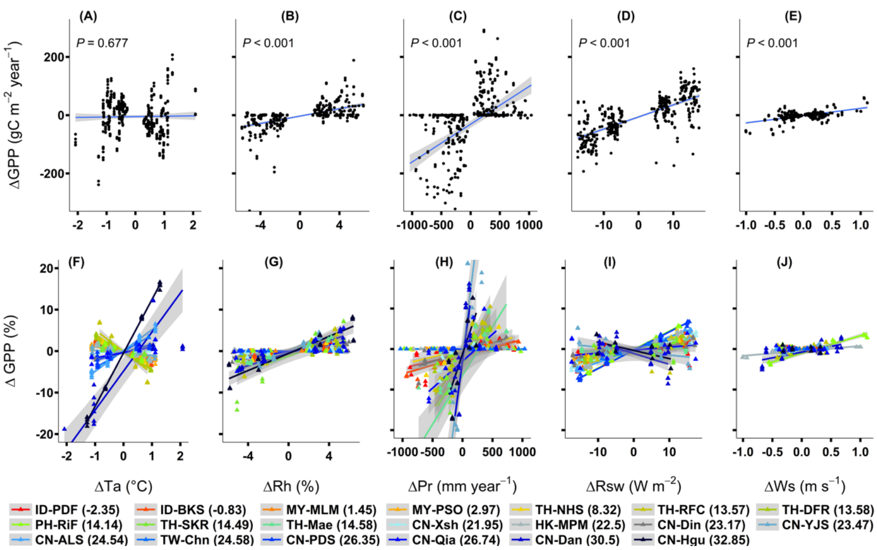

Figure 8. GPP responses to perturbation of various climate drivers, including air temperature, relative humidity, precipitation, short wave radiation, and wind speed. The top panels show the absolute changes of GPP, and the bottom panels show the relative changes of GPP in percentage. The air temperature perturbation with method (iii) is reported to isolate the pure air temperature effect. Note that some of the extreme points beyond the plotting range are not shown for visual clarity; however, all data points were included in the regression fit.

3.5 Sensitivity of WUE to climatic variables in the perturbation experiments

WUE is most sensitive to changes in relative humidity with a range of ±0.5 gC m^{-2} mm^{-1} (±12%) and least sensitive to pure air temperature changes with a range of ±0.125 gC m^{-2} mm^{-1} (±3% for most points, Figure 9). In general, higher relative humidity leads to an increase in WUE across all sites, especially for already wet sites

https://doi.org/10.5194/egusphere-2025-4570
Preprint. Discussion started: 5 October 2025

such as TW-Chn cloud forest and MY-MLM swamp forest. With higher relative humidity, VPD decreases and causes a larger reduction of transpiration (larger than 1.5% per 1% changes in R_h) due to the reduced atmospheric demand but it does not affect considerably stomatal aperture (e.g., Figure S5E and Figure S9E), while its effect on GPP is negligible (<0.01% per 1% changes in R_h, Table S2) as GPP limited by energy, leading to a considerably enhanced WUE.

Air temperature warming (pure, method iii) decreases WUE for most of the sites, with reduced GPP and LAI being the dominant factor except at certain cold sites and sites with standing water (Figure 9F). These sites show an increase in WUE with warmer temperatures but for different reasons. For the colder sites such as CN-Dan and CN-Hgu, warmer temperatures enhance GPP strongly (~10% for 1°C changes in T_a, Table S2) and affect transpiration only slightly (~4%, Table S1). For PH-RiF and HK-MPM, where there is often ponding surface water, warmer temperatures can reduce transpiration (~3.3%) slightly more than GPP (~2%, Table S2), which leads to higher WUE. WUE responses to air temperature changes are different for different methods of perturbing the associate humidity. For the method (ii), all sites show a decreasing trend in WUE (larger than 9% per 1°C changes in T_a) with warming as VPD increases. Results for method (i) shows very small responses (smaller than 4.5% for most sites) to warming (Figure S7, Table S3).

Precipitation changes do not affect (<1% for increase 100 mm year^{-1} increase in P_r) WUE in most tropical and subtropical sites as they are not modifying the water status of plants (Figure 9H, Table S3). For the dry sites (i.e., CN-YJS, CN-Dan, CN-Hgu), WUE increases substantially (> 3.3% for 100 mm year^{-1} increase in P_r) with more precipitation, as this stimulates GPP and LAI with compounding effects on productivity. Higher shortwave radiation decreases WUE for all sites, which is due to

https://doi.org/10.5194/egusphere-2025-4570
Preprint. Discussion started: 5 October 2025

it influencing more transpiration than GPP for humid sites and reducing GPP due to enhanced water stress for dry sites. Higher wind speed generally decreases WUE, which is due to transpiration increasing more than GPP in response to a smaller aerodynamic resistance, except for the dry sites mentioned above. The increase in WUE with higher wind speed in dry sites is due to the increased diffusion of CO_2, which enhances GPP, while at the annual scale transpiration is unchanged as it is largely dictated by precipitation.

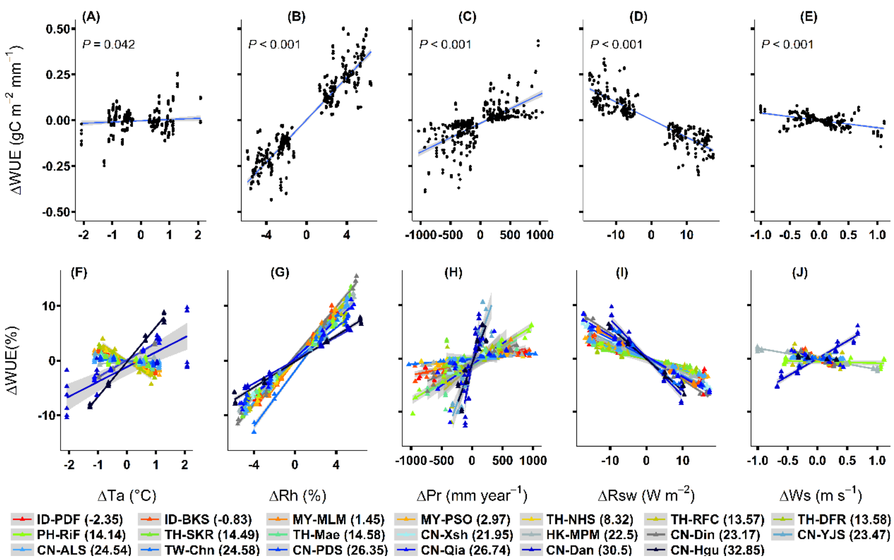

Figure 9. Water use efficiency (WUE, calculated as GPP/Trans) responses to perturbations of climate drivers such as air temperature, relative humidity, precipitation, shortwave radiation, and wind speed. The top panels are absolute changes, and bottom panels are relative changes. The air temperature perturbation with method (iii) is reported to isolate the pure air temperature effect. Note that some of the extreme points beyond the plotting range are not shown for visual clarity; however, all data points were included in the regression fit.

3.6 Sensitivity of CUE to climatic variables in the perturbation experiments

CUE is most sensitive to air temperature changes, with warmer temperatures leading to a lower CUE, which is due to enhanced maintenance respiration with warming (Figure 10A and F). For every 1 °C increase in air temperature, there is more than

https://doi.org/10.5194/egusphere-2025-4570
Preprint. Discussion started: 5 October 2025

1.5% decrease in CUE. The most sensitive sites are the two rubber plantation sites (TH-NHS and TH-RFC) with a 4.7% - 7.4% drop of CUE for every 1 °C increase in air temperature, likely due to their higher allocation to non-structural carbohydrates, while the least responsive one is the CN-Dan in Tibetan plateau, with around 1% drop of CUE, as in there, temperature stimulates GPP as well. Moreover, these patterns are consistent across different perturbation methods of air temperature, which indicates that air temperature changes are the primary driver instead of the VPD changes (Figure S8). Generally, precipitation changes have a small effect (smaller than 0.7% for every 100 mm year^{-1} changes) on CUE, except for the three dry sites (larger than 1.4%, CN-YJS, CN-Dan, CN-Hgu, Figure 10H, Table S4). For these three sites, higher productivity associated with more precipitation leads to higher LAI, a longer active season, and more respiration costs which, however, increase proportionally less than GPP.

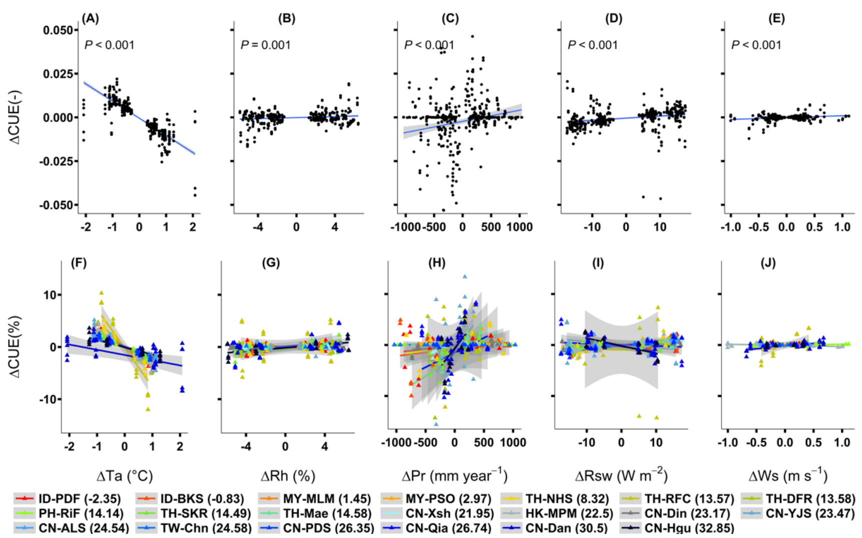

Figure 10. Same as Figure 9 but for carbon use efficiency (CUE), calculated as the ratio between NPP and GPP.

https://doi.org/10.5194/egusphere-2025-4570
Preprint. Discussion started: 5 October 2025

4 Discussion

4.1 An energy-limited region, with exceptions

The presented numerical experiments have shown that ET is most responsive to relative humidity changes, while GPP showed the largest increase in response to higher shortwave radiation (Figure 7B, Figure 8D). However, some dry sites, such as the savanna and Tibetan Plateau grasslands, are water-limited ecosystems and respond primarily to changes in precipitation (Figure 7H, Figure 8H). In summary, our virtual experiments have remarked the degree to which SEA is an energy-limited region, but they have also highlighted strong heterogeneities. For example, the CN-YJS Savanna, despite being in the subtropical region, is highly a water-limited system as compared to the other subtropical evergreen forests. Previous studies have highlighted that a large area of SEA is covered by forest-savannas mosaics (more than 15.5%, Figure 1), underscoring the importance of considering properly these understudied ecosystems in the region (Ratnam et al 2016; Hamilton et al., 2024; Pletcher et al., 2022). Elevation is another critical factor influencing ecosystem responses. For example, TW-Chn and CN-ALS mountain receive much higher amount of precipitation than sites located at similar latitudes and have higher relative humidity and lower solar radiation (Table 2). Consequently, their ET is more energy-limited and exhibits stronger responses to changes in relative humidity and radiation than other subtropical forests (Figure 7,Table S1). Phenology also plays a critical role in determining vegetation responses to climate drivers. Tropical dry deciduous forests (occupying 12.7% of the region) shed their leaves during the dry season as an adaptation strategy to water stress conditions; this is different from subtropical evergreen forests (Reich, 1995; Vico et al., 2015; Zhang et al., 2016). Our study also found that the GPP of dry deciduous forests (e.g., TH-SKR) has a response to precipitation changes stronger

https://doi.org/10.5194/egusphere-2025-4570
Preprint. Discussion started: 5 October 2025

than other subtropical evergreen forests, in turn suggesting that changes in precipitation amount may affect these deciduous forests in a much more significant way than other forests, at least for the precipitation perturbation analysed here spanning 1-2 standard deviation of the interannual variability (Table S2, Figure 8H).

4.2 Limits of interpretation

There are several limitations and sources of uncertainty in our analysis. First, our perturbation experiments did not account for the interactions between different climate drivers, as we perturbed each driver individually. For example, when perturbing the shortwave radiation we did not consider any land-atmospheric feedbacks which may also affect temperature, precipitation, relative humidity and wind speed (Laguë et al., 2019; Wang et al., 2025) The virtual experiments show the opposite effect of increasing shortwave radiation and air temperature on ET and GPP for tropical and subtropical regions (Table S1, Table S2). If the combined effect is considered, the ET and GPP may not respond strongly to radiation changes. Secondly, any of the virtual experiments did not consider the CO_2 fertilization effect that can increase GPP and eventually LAI (Fatichi & Leuzinger, 2013; Yang et al., 2016). Furthermore, we show that warmer temperatures and lower relative humidity both decreased GPP for tropical and subtropical regions. However, higher CO_2 concentrations can buffer this trend with the potential for GPP to not decrease but rather increase in a changing climate. Finally, while representative of many different ecosystems and of the most prominent ecosystems – we analysed only 20 sites, due to availability of meteorological forcing and flux tower data to constrain the model simulations. The public release of existing carbon, water, and energy fluxes dataset in the region (e.g., Kuricheva et al., 2021; Ueyama et al., 2025) or the installation of new flux towers could be fundamental to extend such an analysis in the future.

https://doi.org/10.5194/egusphere-2025-4570
Preprint. Discussion started: 5 October 2025

4.3 Role of humidity and temperature

The virtual experiments have shown that relative humidity (or VPD) perturbations, not the temperature perturbations, are the main driver of ET changes (Figure 7 A&B, Table S1), while temperature changes generally have larger effect than VPD on GPP for tropical and subtropical forests (Figure S6, Table S2). This study shed light on how important is to disentangle the relative role of temperature and VPD on different ecosystems. Temperature and humidity manipulation experiments could shed more light on this aspect, but in the real world, it is challenging to separate temperature and VPD effects in observations because they co-occur. However, it is important to mechanistically understand how ecohydrological fluxes will respond to these two drivers (Zarakas et al., 2024). Recent studies have found that the future cross-correlation of temperature and VPD is non-stationary and can deviate from current relationships because the land ET and moisture transport from ocean to land will not be able to keep pace with the temperature increase over land under global warming (Byrne, 2021; Byrne & O'Gorman, 2016, 2018). Observation studies have found that VPD effects on photosynthesis are stronger than temperature effects in general (Fu et al., 2018; Santos et al., 2018; Slot et al., 2024), but temperature effects are still dominant for GPP in tropical regions (Doughty et al., 2023; Slot & Winter, 2017b, 2017a). The mechanistic ecohydrological simulations presented here corroborate these findings.

5 Conclusions

Through a synthesis of data and mostly mechanistic ecohydrological simulations from 20 available flux tower sites, we found that ET and GPP of SEA locations are strongly energy-limited and only slightly correlated with annual precipitation. The numerical

https://doi.org/10.5194/egusphere-2025-4570
Preprint. Discussion started: 5 October 2025

experiments indicate that ET is highly responsive to changes in relative humidity for tropical and subtropical regions. However, GPP is more responsive to shortwave radiation changes. Warmer temperatures can decrease GPP as the plant thermal optimum for photosynthesis might be exceeded and higher VPD decreases GPP due to its effect on stomata closure. We quantitatively disentangle the relative effect of temperature and humidity and found that the temperature effect is more substantial on GPP. By integrating the flux tower observations and mechanistic modelling studies, we have provided a comprehensive picture of water, energy and carbon fluxes for many major ecosystems of a generally understudied and diverse region as SEA. Spatial heterogeneity within SEA remains evident, and while tropical and subtropical evergreen forests are dominant (~40%), ecoregions such as grasslands in the Tibetan plateau, savannas, and dry deciduous forests occupy ~33% of SEA and behave quite differently, as water-limitations have an important role in their functioning. This study provides deeper insights into the magnitude and environmental factors affecting ecohydrological fluxes across SEA, contributing knowledge to how carbon and water cycle dynamics might change under a future climate.

Code and data availability statement

The reconstructed landcover of Southeast Asia for year 2022 are available in Zenodo: https://doi.org/10.5281/zenodo.16525412 The T&C model code is available at the following link: https://codeocean.com/capsule/0294088/tree/v4.

Author contributions

JR and SF conceived the research idea and designed the study. JR, ZL, and SF collected the data. JR and SF performed model simulations. All authors contributed to the discussion and interpretation of the results. JR led the writing of the manuscript with help from all authors. SF, XL, and SG initiated the projects.

https://doi.org/10.5194/egusphere-2025-4570
Preprint. Discussion started: 5 October 2025

Competing interests

The authors declare that they have no conflict of interest.

Acknowledgements

We acknowledge the support of Singapore's Ministry of Education under its Academic Research Fund Tier 2, Project ID: MOE-000379-00/MOE-000379-01, Award Number: MOE-T2EP50122-0004 and Project ID: MOE-000485-00/ MOE-000485-01, Award Number: MOE-T2EP50222-0006.

References

Aadhar, S., & Mishra, V. (2020). On the Projected Decline in Droughts Over South Asia in CMIP6 Multimodel Ensemble. *Journal of Geophysical Research: Atmospheres*, *125*(20), e2020JD033587. https://doi.org/10.1029/2020JD033587

Alberto, Ma. C. R., Wassmann, R., Hirano, T., Miyata, A., Hatano, R., Kumar, A., et al. (2011). Comparisons of energy balance and evapotranspiration between flooded and aerobic rice fields in the Philippines. *Agricultural Water Management*, *98*(9), 1417–1430. https://doi.org/10.1016/j.agwat.2011.04.011

Alberto, Ma. C. R., Wassmann, R., Buresh, R. J., Quilty, J. R., Correa, T. Q., Sandro, J. M., & Centeno, C. A. R. (2014). Measuring methane flux from irrigated rice fields by eddy covariance method using open-path gas analyzer. *Field Crops Research*, *160*, 12–21. https://doi.org/10.1016/j.fcr.2014.02.008

Bastos, A., O'Sullivan, M., Ciais, P., Makowski, D., Sitch, S., Friedlingstein, P., et al. (2020). Sources of Uncertainty in Regional and Global Terrestrial CO2 Exchange Estimates. *Global Biogeochemical Cycles*, *34*(2), e2019GB006393. https://doi.org/10.1029/2019GB006393

https://doi.org/10.5194/egusphere-2025-4570
Preprint. Discussion started: 5 October 2025

Beer, C., Reichstein, M., Tomelleri, E., Ciais, P., Jung, M., Carvalhais, N., et al. (2010). Terrestrial Gross Carbon Dioxide Uptake: Global Distribution and Covariation with Climate. *Science*, *329*(5993), 834–838. https://doi.org/10.1126/science.1184984

Belton, B., & Fang, P. (2022). Hybrid livelihoods: Maize and agrarian transformation in Southeast Asia's uplands. *Journal of Rural Studies*, *95*, 521–532. https://doi.org/10.1016/j.jrurstud.2022.09.036

Busman, N. A., Melling, L., Goh, K. J., Imran, Y., Sangok, F. E., & Watanabe, A. (2023). Soil CO2 and CH4 fluxes from different forest types in tropical peat swamp forest. *Science of The Total Environment*, *858*, 159973. https://doi.org/10.1016/j.scitotenv.2022.159973

Byrne, M. P. (2021). Amplified warming of extreme temperatures over tropical land. *Nature Geoscience*, *14*(11), 837–841. https://doi.org/10.1038/s41561-021-00828-8

Byrne, M. P., & O'Gorman, P. A. (2016). Understanding Decreases in Land Relative Humidity with Global Warming: Conceptual Model and GCM Simulations. https://doi.org/10.1175/JCLI-D-16-0351.1

Byrne, M. P., & O'Gorman, P. A. (2018). Trends in continental temperature and humidity directly linked to ocean warming. *Proceedings of the National Academy of Sciences*, *115*(19), 4863–4868. https://doi.org/10.1073/pnas.1722312115

Carter, K. R., Cavaleri, M. A., Atkin, O. K., Bahar, N. H. A., Cheesman, A. W., Choury, Z., et al. (2024). Photosynthetic responses to temperature across the tropics: a meta-analytic approach. *Annals of Botany*, mcae206. https://doi.org/10.1093/aob/mcae206

https://doi.org/10.5194/egusphere-2025-4570
Preprint. Discussion started: 5 October 2025

Cervarich, M., Shu, S., Jain, A. K., Arneth, A., Canadell, J., Friedlingstein, P., et al. (2016). The terrestrial carbon budget of South and Southeast Asia. *Environmental Research Letters*, *11*(10), 105006. https://doi.org/10.1088/1748-9326/11/10/105006

Cook, E. R., Anchukaitis, K. J., Buckley, B. M., D'Arrigo, R. D., Jacoby, G. C., & Wright, W. E. (2010). Asian Monsoon Failure and Megadrought During the Last Millennium. *Science*, *328*(5977), 486–489. https://doi.org/10.1126/science.1185188

Damour, G., Simonneau, T., Cochard, H., & Urban, L. (2010). An overview of models of stomatal conductance at the leaf level. *Plant, Cell & Environment*, *33*(9), 1419–1438.

De Lucia, E. H., Drake, J. E., Thomas, R. B., & Gonzalez-Meler, M. (2007). Forest carbon use efficiency: is respiration a constant fraction of gross primary production? *Global Change Biology*, *13*(6), 1157–1167. https://doi.org/10.1111/j.1365-2486.2007.01365.x

Descals, A., Wich, S., Meijaard, E., Gaveau, D. L. A., Peedell, S., & Szantoi, Z. (2021). High-resolution global map of smallholder and industrial closed-canopy oil palm plantations. *Earth System Science Data*, *13*(3), 1211–1231. https://doi.org/10.5194/essd-13-1211-2021

Doughty, C. E., Keany, J. M., Wiebe, B. C., Rey-Sanchez, C., Carter, K. R., Middleby, K. B., et al. (2023). Tropical forests are approaching critical temperature thresholds. *Nature*, *621*(7977), 105–111. https://doi.org/10.1038/s41586-023-06391-z

Estoque, R. C., Ooba, M., Avitabile, V., Hijioka, Y., DasGupta, R., Togawa, T., & Murayama, Y. (2019). The future of Southeast Asia's forests. *Nature Communications*, *10*(1), 1829. https://doi.org/10.1038/s41467-019-09646-4

Fatichi, S., Ivanov, V. Y., & Caporali, E. (2012a). A mechanistic ecohydrological model to investigate complex interactions in cold and warm water-controlled environments: 1. Theoretical framework and plot-scale analysis. *Journal of Advances in Modeling Earth Systems*, *4*(2). https://doi.org/10.1029/2011MS000086

Fatichi, S., Ivanov, V. Y., & Caporali, E. (2012b). A mechanistic ecohydrological model to investigate complex interactions in cold and warm water-controlled environments: 2. Spatiotemporal analyses. *Journal of Advances in Modeling Earth Systems*, *4*(2). https://doi.org/10.1029/2011MS000087

Fatichi, Simone, & Leuzinger, S. (2013). Reconciling observations with modeling: The fate of water and carbon allocation in a mature deciduous forest exposed to elevated CO2. *Agricultural and Forest Meteorology*, *174–175*, 144–157. https://doi.org/10.1016/j.agrformet.2013.02.005

Fatichi, Simone, Zeeman, M. J., Fuhrer, J., & Burlando, P. (2014). Ecohydrological effects of management on subalpine grasslands: From local to catchment scale. *Water Resources Research*, *50*(1), 148–164. https://doi.org/10.1002/2013WR014535

Fatichi, Simone, Paschalis, A., Bonetti, S., Manoli, G., & Pappas, C. (2023). Water use efficiency: A review of spatial and temporal variability. In M. J. Goss & M. Oliver (Eds.), *Encyclopedia of Soils in the Environment (Second Edition)* (pp. 527–542). Oxford: Academic Press. https://doi.org/10.1016/B978-0-12-822974-3.00166-X

https://doi.org/10.5194/egusphere-2025-4570
Preprint. Discussion started: 5 October 2025

Fei, X., Jin, Y., Zhang, Y., Sha, L., Liu, Y., Song, Q., et al. (2017). Eddy covariance and biometric measurements show that a savanna ecosystem in Southwest China is a carbon sink. *Scientific Reports*, *7*(1), 41025. https://doi.org/10.1038/srep41025

Fei, X., Song, Q., Zhang, Y., Liu, Y., Sha, L., Yu, G., et al. (2018). Carbon exchanges and their responses to temperature and precipitation in forest ecosystems in Yunnan, Southwest China. *Science of The Total Environment*, *616–617*, 824–840. https://doi.org/10.1016/j.scitotenv.2017.10.239

Friedl, M. A, McIver, D. K., Hodges, J. C. F., Zhang, X. Y., Muchoney, D., Strahler, A. H., et al. (2002). Global land cover mapping from MODIS: algorithms and early results. *Remote Sensing of Environment*, *83*(1), 287–302. https://doi.org/10.1016/S0034-4257(02)00078-0

Friedl, Mark A., Sulla-Menashe, D., Tan, B., Schneider, A., Ramankutty, N., Sibley, A., & Huang, X. (2010). MODIS Collection 5 global land cover: Algorithm refinements and characterization of new datasets. *Remote Sensing of Environment*, *114*(1), 168–182. https://doi.org/10.1016/j.rse.2009.08.016

Fu, Z., Gerken, T., Bromley, G., Araújo, A., Bonal, D., Burban, B., et al. (2018). The surface-atmosphere exchange of carbon dioxide in tropical rainforests: Sensitivity to environmental drivers and flux measurement methodology. *Agricultural and Forest Meteorology*, *263*, 292–307. https://doi.org/10.1016/j.agrformet.2018.09.001

Funk, C., Peterson, P., Landsfeld, M., Pedreros, D., Verdin, J., Shukla, S., et al. (2015). The climate hazards infrared precipitation with stations—a new environmental record for monitoring extremes. *Scientific Data*, *2*(1), 150066. https://doi.org/10.1038/sdata.2015.66

https://doi.org/10.5194/egusphere-2025-4570
Preprint. Discussion started: 5 October 2025

GAMO, M. (2005). Carbon flux observation in the tropical seasonal forests and tropical rain forest. *Proceedings of the International Workshop on Advanced Flux Network and Flux Evaluation (AsiaFlux Workshop 2005), Fujiyoshida*, *86*. Retrieved from https://cir.nii.ac.jp/crid/1570291224383367936

Giambelluca, T. W., Mudd, R. G., Liu, W., Ziegler, A. D., Kobayashi, N., Kumagai, T., et al. (2016). Evapotranspiration of rubber (Hevea brasiliensis) cultivated at two plantation sites in Southeast Asia. *Water Resources Research*, *52*(2), 660–679. https://doi.org/10.1002/2015WR017755

Grossiord, C., Bachofen, C., Gisler, J., Mas, E., Vitasse, Y., & Didion-Gency, M. (2022). Warming may extend tree growing seasons and compensate for reduced carbon uptake during dry periods. *Journal of Ecology*, *110*(7), 1575–1589. https://doi.org/10.1111/1365-2745.13892

Guan, K., Pan, M., Li, H., Wolf, A., Wu, J., Medvigy, D., et al. (2015). Photosynthetic seasonality of global tropical forests constrained by hydroclimate. *Nature Geoscience*, *8*(4), 284–289. https://doi.org/10.1038/ngeo2382

Hamilton, R., Amano, N., Bradshaw, C. J. A., Saltré, F., Patalano, R., Penny, D., et al. (2024). Forest mosaics, not savanna corridors, dominated in Southeast Asia during the Last Glacial Maximum. *Proceedings of the National Academy of Sciences*, *121*(1), e2311280120. https://doi.org/10.1073/pnas.2311280120

Hansen, M. C., Potapov, P. V., Moore, R., Hancher, M., Turubanova, S. A., Tyukavina, A., et al. (2013). High-Resolution Global Maps of 21st-Century Forest Cover Change. *Science*, *342*(6160), 850–853.

Hersbach, H., Bell, B., Berrisford, P., Hirahara, S., Horányi, A., Muñoz-Sabater, J., et al. (2020). The ERA5 global reanalysis. *Quarterly Journal of the Royal Meteorological Society*, *146*(730), 1999–2049. https://doi.org/10.1002/qj.3803

https://doi.org/10.5194/egusphere-2025-4570
Preprint. Discussion started: 5 October 2025

Hirano, T., Segah, H., Harada, T., Limin, S., June, T., Hirata, R., & Osaki, M. (2007). Carbon dioxide balance of a tropical peat swamp forest in Kalimantan, Indonesia. *Global Change Biology*, *13*(2), 412–425. https://doi.org/10.1111/j.1365-2486.2006.01301.x

Hirata, R., Saigusa, N., Yamamoto, S., Ohtani, Y., Ide, R., Asanuma, J., et al. (2008). Spatial distribution of carbon balance in forest ecosystems across East Asia. *Agricultural and Forest Meteorology*, *148*(5), 761–775. https://doi.org/10.1016/j.agrformet.2007.11.016

Hsieh, C.-I., Lai, M.-C., Hsia, Y.-J., & Chang, T.-J. (2008). Estimation of sensible heat, water vapor, and CO2 fluxes using the flux-variance method. *International Journal of Biometeorology*, *52*(6), 521–533. https://doi.org/10.1007/s00484-008-0149-4

Huang, M., Piao, S., Ciais, P., Peñuelas, J., Wang, X., Keenan, T. F., et al. (2019). Air temperature optima of vegetation productivity across global biomes. *Nature Ecology & Evolution*, *3*(5), 772–779. https://doi.org/10.1038/s41559-019-0838-x

Huete, A. R., Restrepo-Coupe, N., Ratana, P., Didan, K., Saleska, S. R., Ichii, K., et al. (2008). Multiple site tower flux and remote sensing comparisons of tropical forest dynamics in Monsoon Asia. *Agricultural and Forest Meteorology*, *148*(5), 748–760. https://doi.org/10.1016/j.agrformet.2008.01.012

Ichii, K., Ueyama, M., Kondo, M., Saigusa, N., Kim, J., Alberto, Ma. C., et al. (2017). New data-driven estimation of terrestrial CO2 fluxes in Asia using a standardized database of eddy covariance measurements, remote sensing data, and support vector regression. *Journal of Geophysical Research: Biogeosciences*, *122*(4), 767–795. https://doi.org/10.1002/2016JG003640

https://doi.org/10.5194/egusphere-2025-4570
Preprint. Discussion started: 5 October 2025

Igarashi, Y., Kumagai, T., Yoshifuji, N., Sato, T., Tanaka, N., Tanaka, K., et al. (2015). Environmental control of canopy stomatal conductance in a tropical deciduous forest in northern Thailand. *Agricultural and Forest Meteorology*, *202*, 1–10. https://doi.org/10.1016/j.agrformet.2014.11.013

Kanpanon, N., Kasemsap, P., Thaler, P., Kositsup, B., Gay, F., Lacote, R., & Epron, D. (2015). Carbon isotope composition of latex does not reflect temporal variations of photosynthetic carbon isotope discrimination in rubber trees (Hevea brasiliensis). *Tree Physiology*, *35*(11), 1166–1175. https://doi.org/10.1093/treephys/tpv070

Kato, T., & Tang, Y. (2008). Spatial variability and major controlling factors of CO2 sink strength in Asian terrestrial ecosystems: evidence from eddy covariance data. *Global Change Biology*, *14*(10), 2333–2348. https://doi.org/10.1111/j.1365-2486.2008.01646.x

Kuricheva, O. A., Avilov, V. K., Dinh, D. B., Sandlersky, R. B., Kuznetsov, A. N., & Kurbatova, J. A. (2021). Seasonality of energy and water fluxes in a tropical moist forest in Vietnam. *Agricultural and Forest Meteorology*, *298–299*, 108268. https://doi.org/10.1016/j.agrformet.2020.108268

Laguë, M. M., Bonan, G. B., & Swann, A. L. (2019). Separating the impact of individual land surface properties on the terrestrial surface energy budget in both the coupled and uncoupled land–atmosphere system. *Journal of Climate*, *32*(18), 5725–5744.

Lavers, D. A., Simmons, A., Vamborg, F., & Rodwell, M. J. (2022). An evaluation of ERA5 precipitation for climate monitoring. *Quarterly Journal of the Royal Meteorological Society*, *148*(748), 3152–3165. https://doi.org/10.1002/qj.4351

https://doi.org/10.5194/egusphere-2025-4570
Preprint. Discussion started: 5 October 2025

Li, Z., Zhang, Y., Wang, S., Yuan, G., Yang, Y., & Cao, M. (2010). Evapotranspiration of a tropical rain forest in Xishuangbanna, southwest China. *Hydrological Processes*, *24*(17), 2405–2416. https://doi.org/10.1002/hyp.7643

Liu, J., & Lai, D. Y. F. (2019). Subtropical mangrove wetland is a stronger carbon dioxide sink in the dry than wet seasons. *Agricultural and Forest Meteorology*, *278*, 107644. https://doi.org/10.1016/j.agrformet.2019.107644

Liu, J., Ryu, Y., Luo, X., Dechant, B., Stocker, B. D., Keenan, T. F., et al. (2024). Evidence for widespread thermal acclimation of canopy photosynthesis. *Nature Plants*, *10*(12), 1919–1927. https://doi.org/10.1038/s41477-024-01846-1

Luo, X., Zhao, R., Chu, H., Collalti, A., Fatichi, S., Keenan, T. F., et al. (2025). Global variation in vegetation carbon use efficiency inferred from eddy covariance observations. *Nature Ecology & Evolution*, 1–12. https://doi.org/10.1038/s41559-025-02753-0

Luo, Z., Ren, J., Manzoni, S., & Fatichi, S. (2024). Temperature controls the relation between soil organic carbon and microbial carbon use efficiency. *Global Change Biology*, *30*(9), e17492. https://doi.org/10.1111/gcb.17492

Manoli, G., Meijide, A., Huth, N., Knohl, A., Kosugi, Y., Burlando, P., et al. (2018). Ecohydrological changes after tropical forest conversion to oil palm. *Environmental Research Letters*, *13*(6), 064035. https://doi.org/10.1088/1748-9326/aac54e

Mastrotheodoros, T., Pappas, C., Molnar, P., Burlando, P., Hadjidoukas, P., & Fatichi, S. (2019). Ecohydrological dynamics in the Alps: Insights from a modelling analysis of the spatial variability. *Ecohydrology*, *12*(1), e2054. https://doi.org/10.1002/eco.2054

https://doi.org/10.5194/egusphere-2025-4570
Preprint. Discussion started: 5 October 2025

Meili, N., Beringer, J., Zhao, J., & Fatichi, S. (2024). Aerodynamic effects cause higher forest evapotranspiration and water yield reductions after wildfires in tall forests. *Global Change Biology*, *30*(1), e16995. https://doi.org/10.1111/gcb.16995

Moustakis, Y., Fatichi, S., Onof, C., & Paschalis, A. (2022). Insensitivity of Ecosystem Productivity to Predicted Changes in Fine-Scale Rainfall Variability. *Journal of Geophysical Research: Biogeosciences*, *127*(2), e2021JG006735. https://doi.org/10.1029/2021JG006735

Nguyen, H. T. T., Turner, S. W. D., Buckley, B. M., & Galelli, S. (2020). Coherent Streamflow Variability in Monsoon Asia Over the Past Eight Centuries—Links to Oceanic Drivers. *Water Resources Research*, *56*(12), e2020WR027883. https://doi.org/10.1029/2020WR027883

Novick, K. A., Ficklin, D. L., Grossiord, C., Konings, A. G., Martínez-Vilalta, J., Sadok, W., et al. (2024). The impacts of rising vapour pressure deficit in natural and managed ecosystems. *Plant, Cell & Environment*, *47*(9), 3561–3589. https://doi.org/10.1111/pce.14846

Oliver, R. J., Mercado, L. M., Medlyn, B. E., Harris, P. P., & Clark, D. B. (2025). Contrasting Impacts of Acclimation and Adaptation of Photosynthetic Capacity to Temperature and CO2 Across Biomes. *Global Biogeochemical Cycles*, *39*(7), e2024GB008398. https://doi.org/10.1029/2024GB008398

Pappas, C., Fatichi, S., & Burlando, P. (2016). Modeling terrestrial carbon and water dynamics across climatic gradients: does plant trait diversity matter? *New Phytologist*, *209*(1), 137–151. https://doi.org/10.1111/nph.13590

https://doi.org/10.5194/egusphere-2025-4570
Preprint. Discussion started: 5 October 2025

Paschalis, A., De Kauwe, M. G., Sabot, M., & Fatichi, S. (2024). When do plant hydraulics matter in terrestrial biosphere modelling? *Global Change Biology*, *30*(1), e17022. https://doi.org/10.1111/gcb.17022

Pastorello, G., Trotta, C., Canfora, E., Chu, H., Christianson, D., Cheah, Y.-W., et al. (2020). The FLUXNET2015 dataset and the ONEFlux processing pipeline for eddy covariance data. *Scientific Data*, *7*(1), 225. https://doi.org/10.1038/s41597-020-0534-3

Peng, H., Chi, J., Yao, H., Guo, Q., Hong, B., Ding, H., et al. (2021). Methane Emissions Offset Net Carbon Dioxide Uptake From an Alpine Peatland on the Eastern Qinghai-Tibetan Plateau. *Journal of Geophysical Research: Atmospheres*, *126*(19), e2021JD034671. https://doi.org/10.1029/2021JD034671

Pletcher, E., Staver, C., & Schwartz, N. B. (2022). The environmental drivers of tree cover and forest–savanna mosaics in Southeast Asia. *Ecography*, *2022*(8), e06280. https://doi.org/10.1111/ecog.06280

Potapov, P., Turubanova, S., Hansen, M. C., Tyukavina, A., Zalles, V., Khan, A., et al. (2022). Global maps of cropland extent and change show accelerated cropland expansion in the twenty-first century. *Nature Food*, *3*(1), 19–28. https://doi.org/10.1038/s43016-021-00429-z

Qian, X., Qiu, B., & Zhang, Y. (2019). Widespread Decline in Vegetation Photosynthesis in Southeast Asia Due to the Prolonged Drought During the 2015/2016 El Niño. *Remote Sensing*, *11*(8), 910. https://doi.org/10.3390/rs11080910

Ratnam, J., Tomlinson, K. W., Rasquinha, D. N., & Sankaran, M. (2016). Savannahs of Asia: antiquity, biogeography, and an uncertain future. *Philosophical*

https://doi.org/10.5194/egusphere-2025-4570
Preprint. Discussion started: 5 October 2025

Transactions of the Royal Society B: Biological Sciences, *371*(1703), 20150305. https://doi.org/10.1098/rstb.2015.0305

Reich, P. B. (1995). Phenology of tropical forests: patterns, causes, and consequences. *Canadian Journal of Botany*, *73*(2), 164–174. https://doi.org/10.1139/b95-020

Sabot, M. E. B., De Kauwe, M. G., Pitman, A. J., Medlyn, B. E., Ellsworth, D. S., Martin-StPaul, N. K., et al. (2022). One Stomatal Model to Rule Them All? Toward Improved Representation of Carbon and Water Exchange in Global Models. *Journal of Advances in Modeling Earth Systems*, *14*(4), e2021MS002761. https://doi.org/10.1029/2021MS002761

Saigusa, N., Yamamoto, S., Hirata, R., Ohtani, Y., Ide, R., Asanuma, J., et al. (2008). Temporal and spatial variations in the seasonal patterns of CO2 flux in boreal, temperate, and tropical forests in East Asia. *Agricultural and Forest Meteorology*, *148*(5), 700–713. https://doi.org/10.1016/j.agrformet.2007.12.006

Sakai, A. (2019). Brief communication: Updated GAMDAM glacier inventory over high-mountain Asia. *The Cryosphere*, *13*(7), 2043–2049. https://doi.org/10.5194/tc-13-2043-2019

Santos, V. A. H. F. D., Ferreira, M. J., Rodrigues, J. V. F. C., Garcia, M. N., Ceron, J. V. B., Nelson, B. W., & Saleska, S. R. (2018). Causes of reduced leaf-level photosynthesis during strong El Niño drought in a Central Amazon forest. *Global Change Biology*, *24*(9), 4266–4279. https://doi.org/10.1111/gcb.14293

Sanwangsri, M., Hanpattanakit, P., & Chidthaisong, A. (2017). Variations of Energy Fluxes and Ecosystem Evapotranspiration in a Young Secondary Dry Dipterocarp Forest in Western Thailand. *Atmosphere*, *8*(8), 152. https://doi.org/10.3390/atmos8080152

https://doi.org/10.5194/egusphere-2025-4570
Preprint. Discussion started: 5 October 2025

Satriawan, T. W., Luo, X., Tian, J., Ichii, K., Juneng, L., & Kondo, M. (2024). Strong Green-Up of Tropical Asia During the 2015/16 El Niño. *Geophysical Research Letters*, *51*(8), e2023GL106955. https://doi.org/10.1029/2023GL106955

Shi, P., Sun, X., Xu, L., Zhang, X., He, Y., Zhang, D., & Yu, G. (2006). Net ecosystem CO2 exchange and controlling factors in a steppe—Kobresia meadow on the Tibetan Plateau. *Science in China Series D: Earth Sciences*, *49*(S2), 207–218. https://doi.org/10.1007/s11430-006-8207-4

Sirisena, T. A. J. G., Maskey, S., Ranasinghe, R., & Babel, M. S. (2018). Effects of different precipitation inputs on streamflow simulation in the Irrawaddy River Basin, Myanmar. *Journal of Hydrology: Regional Studies*, *19*, 265–278. https://doi.org/10.1016/j.ejrh.2018.10.005

Slot, M., & Winter, K. (2017a). In situ temperature relationships of biochemical and stomatal controls of photosynthesis in four lowland tropical tree species. *Plant, Cell & Environment*, *40*(12), 3055–3068. https://doi.org/10.1111/pce.13071

Slot, M., & Winter, K. (2017b). In situ temperature response of photosynthesis of 42 tree and liana species in the canopy of two Panamanian lowland tropical forests with contrasting rainfall regimes. *New Phytologist*, *214*(3), 1103–1117. https://doi.org/10.1111/nph.14469

Slot, M., Rifai, S. W., Eze, C. E., & Winter, K. (2024). The stomatal response to vapor pressure deficit drives the apparent temperature response of photosynthesis in tropical forests. *New Phytologist*, *244*(4), 1238–1249. https://doi.org/10.1111/nph.19806

Smith, M. N., Taylor, T. C., van Haren, J., Rosolem, R., Restrepo-Coupe, N., Adams, J., et al. (2020). Empirical evidence for resilience of tropical forest

https://doi.org/10.5194/egusphere-2025-4570
Preprint. Discussion started: 5 October 2025

photosynthesis in a warmer world. *Nature Plants*, *6*(10), 1225–1230. https://doi.org/10.1038/s41477-020-00780-2

Song, Q.-H., Braeckevelt, E., Zhang, Y.-P., Sha, L.-Q., Zhou, W.-J., Liu, Y.-T., et al. (2017). Evapotranspiration from a primary subtropical evergreen forest in Southwest China. *Ecohydrology*, *10*(4), e1826. https://doi.org/10.1002/eco.1826

Stott, P. (1990). Stability and Stress in the Savanna Forests of Mainland South-East Asia. *Journal of Biogeography*, *17*(4/5), 373. https://doi.org/10.2307/2845366

Sullivan, M. J. P., Lewis, S. L., Affum-Baffoe, K., Castilho, C., Costa, F., Sanchez, A. C., et al. (2020). Long-term thermal sensitivity of Earth's tropical forests. *Science*, *368*(6493), 869–874. https://doi.org/10.1126/science.aaw7578

Sun, C., Zhang, H., Xu, L., Ge, J., Jiang, J., Zuo, L., & Wang, C. (2023). Twenty-meter annual paddy rice area map for mainland Southeast Asia using Sentinel-1 synthetic-aperture-radar data. *Earth System Science Data*, *15*(4), 1501–1520. https://doi.org/10.5194/essd-15-1501-2023

Takanashi, S., Kosugi, Y., Ohkubo, S., Matsuo, N., Tani, M., & Nik, A. R. (2010). Water and heat fluxes above a lowland dipterocarp forest in Peninsular Malaysia. *Hydrological Processes*, *24*(4), 472–480. https://doi.org/10.1002/hyp.7499

Tan, Z.-H., Zhang, Y.-P., Liang, N., Hsia, Y.-J., Zhang, Y.-J., Zhou, G.-Y., et al. (2012). An observational study of the carbon-sink strength of East Asian subtropical evergreen forests. *Environmental Research Letters*, *7*(4), 044017. https://doi.org/10.1088/1748-9326/7/4/044017

Tan, Z.-H., Zeng, J., Zhang, Y.-J., Slot, M., Gamo, M., Hirano, T., et al. (2017). Optimum air temperature for tropical forest photosynthesis: mechanisms

https://doi.org/10.5194/egusphere-2025-4570
Preprint. Discussion started: 5 October 2025

involved and implications for climate warming. *Environmental Research Letters*, *12*(5), 054022. https://doi.org/10.1088/1748-9326/aa6f97

Tanaka, N., Kume, T., Yoshifuji, N., Tanaka, K., Takizawa, H., Shiraki, K., et al. (2008). A review of evapotranspiration estimates from tropical forests in Thailand and adjacent regions. *Agricultural and Forest Meteorology*, *148*(5), 807–819. https://doi.org/10.1016/j.agrformet.2008.01.011

Tang, A. C. I., Stoy, P. C., Hirata, R., Musin, K. K., Aeries, E. B., Wenceslaus, J., & Melling, L. (2018). Eddy Covariance Measurements of Methane Flux at a Tropical Peat Forest in Sarawak, Malaysian Borneo. *Geophysical Research Letters*, *45*(9), 4390–4399. https://doi.org/10.1029/2017GL076457

Thirumalai, K., DiNezio, P. N., Okumura, Y., & Deser, C. (2017). Extreme temperatures in Southeast Asia caused by El Niño and worsened by global warming. *Nature Communications*, *8*(1), 15531. https://doi.org/10.1038/ncomms15531

Ueyama, M., Takao, Y., Yazawa, H., Tanaka, M., Yabuki, H., Kumagai, T., et al. (2025). The JapanFlux2024 dataset for eddy covariance observations covering Japan and East Asia from 1990 to 2023. *Earth System Science Data*, *17*(8), 3807–3833. https://doi.org/10.5194/essd-17-3807-2025

Unjan, R., Nissapa, A., & Chiarawipa, R. (2017). Climatic considerations which support the choice between natural rubber and oil palm in Nakhon Si Thammarat, southern Thailand. *Kasetsart Journal of Social Sciences*, *38*(3), 273–281. https://doi.org/10.1016/j.kjss.2016.07.006

Vico, G., Thompson, S. E., Manzoni, S., Molini, A., Albertson, J. D., Almeida-Cortez, J. S., et al. (2015). Climatic, ecophysiological, and phenological controls on

https://doi.org/10.5194/egusphere-2025-4570
Preprint. Discussion started: 5 October 2025

plant ecohydrological strategies in seasonally dry ecosystems. *Ecohydrology*, *8*(4), 660–681. https://doi.org/10.1002/eco.1533

Vijay, V., Pimm, S. L., Jenkins, C. N., & Smith, S. J. (2016). The Impacts of Oil Palm on Recent Deforestation and Biodiversity Loss. *PLOS ONE*, *11*(7), e0159668. https://doi.org/10.1371/journal.pone.0159668

Vu, D. T., Dang, T. D., Pianosi, F., & Galelli, S. (2023). Calibrating macroscale hydrological models in poorly gauged and heavily regulated basins. *Hydrology and Earth System Sciences*, *27*(19), 3485–3504. https://doi.org/10.5194/hess-27-3485-2023

Wang, B. (2006). *The Asian Monsoon*. Springer Science & Business Media. Retrieved from https://link.springer.com/book/10.1007/3-540-37722-0

Wang, C., Yu, G., Zhou, G., Yan, J., Zhang, L., Wang, X., et al. (2006). CO2 flux evaluation over the evergreen coniferous and broad-leaved mixed forest in Dinghushan, China. *Science in China Series D: Earth Sciences*, *49*(2), 127–138. https://doi.org/10.1007/s11430-006-8127-3

Wang, X., Blanken, P. D., Kasemsap, P., Petchprayoon, P., Thaler, P., Nouvellon, Y., et al. (2022). Carbon and Water Cycling in Two Rubber Plantations and a Natural Forest in Mainland Southeast Asia. *Journal of Geophysical Research: Biogeosciences*, *127*(5), e2022JG006840. https://doi.org/10.1029/2022JG006840

Wang, Yanwei, Luo, W., Zeng, G., Peng, H., Cheng, A., Zhang, L., et al. (2020). Characteristics of carbon, water, and energy fluxes on abandoned farmland revealed by critical zone observation in the karst region of southwest China. *Agriculture, Ecosystems & Environment*, *292*, 106821. https://doi.org/10.1016/j.agee.2020.106821

https://doi.org/10.5194/egusphere-2025-4570
Preprint. Discussion started: 5 October 2025

Wang, Yiran, Meili, N., & Fatichi, S. (2025). Ecohydrological responses to solar radiation changes. *Hydrology and Earth System Sciences*, *29*(2), 381–396. https://doi.org/10.5194/hess-29-381-2025

Wang, Yunxia, Hollingsworth, P. M., Zhai, D., West, C. D., Green, J. M. H., Chen, H., et al. (2023). High-resolution maps show that rubber causes substantial deforestation. *Nature*, 1–7. https://doi.org/10.1038/s41586-023-06642-z

Xu, H., Zhang, Z., Wu, X., & Wan, J. (2023). Light use efficiency models incorporating diffuse radiation impacts for simulating terrestrial ecosystem gross primary productivity: A global comparison. *Agricultural and Forest Meteorology*, *332*, 109376. https://doi.org/10.1016/j.agrformet.2023.109376

Xu, Y., Yu, L., Li, W., Ciais, P., Cheng, Y., & Gong, P. (2020). Annual oil palm plantation maps in Malaysia and Indonesia from 2001 to 2016. *Earth System Science Data*, *12*(2), 847–867. https://doi.org/10.5194/essd-12-847-2020

Yang, L.-Y., Yu, R., Wu, J., Zhang, Y., Kosugi, Y., Restrepo-Coupe, N., et al. (2023). Asian tropical forests assimilating carbon under dry conditions: water stress or light benefits? *Journal of Plant Ecology*, *16*(3), rtac106. https://doi.org/10.1093/jpe/rtac106

Yang, Y., Donohue, R. J., McVicar, T. R., Roderick, M. L., & Beck, H. E. (2016). Long-term CO2 fertilization increases vegetation productivity and has little effect on hydrological partitioning in tropical rainforests. *Journal of Geophysical Research: Biogeosciences*, *121*(8), 2125–2140. https://doi.org/10.1002/2016JG003475

You, L., Wood, S., Wood-Sichra, U., & Wu, W. (2014). Generating global crop distribution maps: From census to grid. *Agricultural Systems*, *127*, 53–60. https://doi.org/10.1016/j.agsy.2014.01.002

https://doi.org/10.5194/egusphere-2025-4570
Preprint. Discussion started: 5 October 2025

Yu, G., Song, X., Wang, Q., Liu, Y., Guan, D., Yan, J., et al. (2008). Water-use efficiency of forest ecosystems in eastern China and its relations to climatic variables. *New Phytologist*, *177*(4), 927–937. https://doi.org/10.1111/j.1469-8137.2007.02316.x

Zarakas, C. M., Swann, A. L. S., Koven, C. D., Smith, M. N., & Taylor, T. C. (2024). Different model assumptions about plant hydraulics and photosynthetic temperature acclimation yield diverging implications for tropical forest gross primary production under warming. *Global Change Biology*, *30*(9), e17449. https://doi.org/10.1111/gcb.17449

Zhang, Yiping, Sha, L., Yu, G., Song, Q., Tang, J., Yang, X., et al. (2006). Annual variation of carbon flux and impact factors in the tropical seasonal rain forest of xishuangbanna, SW China. *Science in China Series D: Earth Sciences*, *49*(2), 150–162. https://doi.org/10.1007/s11430-006-8150-4

Zhang, Yuan, Zhu, Z., Liu, Z., Zeng, Z., Ciais, P., Huang, M., et al. (2016). Seasonal and interannual changes in vegetation activity of tropical forests in Southeast Asia. *Agricultural and Forest Meteorology*, *224*, 1–10. https://doi.org/10.1016/j.agrformet.2016.04.009

Zhao, R., Luo, X., Yang, Y., Nurlaila Syahid, L., Chen, C., & Huay Lee, J. S. (2024). Cropland expansion drives vegetation greenness decline in Southeast Asia. *Biogeosciences*, *21*(23), 5393–5406. https://doi.org/10.5194/bg-21-5393-2024